The Coastal Protection Potential of Nature-based Solutions in the Dutch Wadden Sea

Hajna Júlia Tijssen

MSc Thesis in Climate Studies

March 2023

Picture: (Natuurmonumenten, n.d.)

Supervisor: Prof. Dr. JRM (Rob) Alkemade

Environmental System Analysis Group

WAGENINGEN
UNIVERSITY & RESEARCH

The Coastal Protection Potential of Nature-based Solutions in the Dutch Wadden Sea

Hajna Júlia Tijssen

MSc Thesis in Climate Studies

March 2023

Supervisor:
Prof. Dr. JRM (Rob) Alkemade

Examiner:
Solen le Clech'

Wageningen University

Chair Group: Environmental Systems Analysis
Course code: ESA80436

Preface and Acknowledgments

This is the MSc thesis report '*The Coastal Protection Potential of Nature-Based Solutions in the Dutch Wadden Sea*'. It has been written to fulfil the graduation requirements of the MSc Climate studies at Wageningen University, under the guidance of the Environmental Systems Analysis chair group. The research was performed from September 2022 till March 2023.

When starting the process of choosing a topic for my thesis I knew I wanted to do something that linked biodiversity with climate adaptation. When approaching Rob with this idea, he mentioned the just-started collaboration in an international research project "*Solving the Sustainability Challenges at the Food-Climate-Biodiversity Nexus*". One of the goals of this project is to find how biodiversity can be managed to support climate adaptation.

From this context and after a discussion with Rob, we arrived at the idea to look at Nature-based Solutions (NbS) and how these can help with climate adaptation. As I wanted to work on an issue relevant to the Netherlands, the idea to look at the relation between Nature-based Solutions and coastal protection appeared. From here, the research formed itself into the context that this report has been written in, which you will shortly discover. But first, I would like to thank several people without whom this research would not have been possible.

First, I would like to express my sincere gratitude to my supervisor Prof. Dr. JRM (Rob) Alkemade. He has helped with shaping the direction of this thesis with his continuous feedback and support. His ideas and suggestions were crucial for this research and I am very grateful for all his help. I am also looking forward to our further collaboration, as Rob will supervise the internship I am starting at Climate Cleanup.

Secondly, this research would not have been possible without the technical support of Reiner Schrijvershof. By providing his model created for the Ems-Dollard estuary in Delft3D-FM, he made the modelling of NbS within this setting possible. Moreover, his guidance with the use of this model was crucial in overcoming moments when the research would otherwise have been stuck.

Thirdly, I would like to thank Solen le Clech' for her feedback on the research proposal and for accepting to be the examiner of this thesis. I am looking forward to her feedback on this final report.

Additionally, I would like to thank the reviewers of this report, who have helped with finding the mistakes I overlooked. Thank you, Hein Hottentot and Márta Domokos.

And lastly, I would like to thank you, my reader, I hope you enjoy your reading and find something of interest to you.

Hajna Julia Tijssen,

Wageningen, 31 March, 2023

Abstract

Coastal areas are highly biodiverse but vulnerable systems. With predicted sea level rise (SLR) due to climate change, there is an increasing need for coastal adaptation to protect coastal systems from flooding and erosion. Conventional coastal engineering solutions are increasingly challenged by SLR and the constant maintenance that is needed to keep up with the changing conditions. Because of their natural adaptability, Nature-based Solutions (NbS) have been recognised as alternative ways for coastal protection. In the Wadden Sea in the Netherlands several NbS for coastal protection are present, for example, salt marshes, seagrasses and oyster reefs. However, the Wadden Sea is a low-lying and continually changing coastal area which is particularly vulnerable to climate change and SLR. Therefore, this thesis aims to identify to what extent NbS can contribute to coastal protection in the Dutch Wadden Sea in the current situation and with SLR by the year 2100. A depth-averaged hydrodynamic model, the Delft3D Flexible Mesh Flow module, was used to simulate the effect of NbS on coastal protection. Within this model the trachytope functionality with the Baptist (2007) method was used to model how the presence of salt marsh (*Spartina anglica*), seagrass (*Zostera marina* and *Zostera noltii*), and oyster (*Ostrea edulis*) species influences the flow velocity, water depth and level of erosion. NbS were studied in the Uithuizerwad and Groningerwad area, and the hydrodynamics were modelled for the whole Ems-Dollard estuary. The bed shear stress was studied as a proxy for the level of erosion. Furthermore, different Representative Concentration Pathway (RCP) SLR scenarios were simulated by 2100. The results show that the salt marsh and seagrass species decrease the daily peak flow velocity by 70%, the peak water depth by 6-34% (depending on location) and the bed shear stress by 80-90% at the coast. The oyster reefs resulted in a decline of 12% in the peak flow velocity, 5-8% in the water depth and 40-60% in the bed shear stress. This indicates that seagrass and salt marsh species are more effective in buffering hydrodynamic forces in front of the coast than oyster reefs. The height of the NbS was found to be the determining factor for the coastal protection potential, while the density and drag coefficient to a lesser extent. With SLR, the NbS decreased the flow velocity, but only a small decrease in the peak water level was found. Furthermore, the period of inundation increased. This indicates that NbS can help with coastal protection in the Dutch Wadden Sea, but their effectiveness is dependent on their properties and the hydrodynamic conditions they are present in. Therefore, a hybrid approach to coastal protection, by combining NbS with conventional coastal engineering solutions, seems to be the best way forward for the Wadden Sea. Further research is needed to determine how SLR and the increased inundation period will impact NbS and the coastal protection they provide.

Table of Contents

1. Introduction

1.1. General background

Coastal systems are highly dynamic and biodiverse systems, but are being threatened by multiple anthropogenic pressures (Agardy et al., 2005). Coastal systems are near-shore areas on land and in the sea, and areas where fresh- and saltwater mix (e.g., estuaries). Coastal areas are home to highly productive and biodiverse ecosystems, such as mangroves, salt marshes and reefs. These ecosystems offer a disproportionately high amount of ecosystem services compared to other systems; which are contributions society receives from natural systems (Agardy et al., 2005; Haines-Young & Potschin, 2017). Nearly 40% of the global population lives within 100 km from the shoreline (Agardy et al., 2005). The continually increasing population is enhancing the pressures on coastal ecosystems. Such pressures include overexploitation of ecosystems, urbanisation, pollution and climate change (Agardy et al., 2005; Wong et al., 2014).

Climate change is increasing the vulnerability of coastal systems. The main pressure from climate change on coastal zones is sea level rise (hereafter SLR), with adverse impacts such as coastal flooding, submergence, and erosion (Pörtner et al., 2019; Wong et al., 2014). Moreover, increasing ocean temperatures and acidification are also affecting coastal ecosystems (Wong et al., 2014).

With 26% of its landmass already below sea level, and a more than 500 km long coastline, the Netherlands is a country highly susceptible to SLR (Pieterse et al., 2009). If greenhouse gas emissions are not reduced, it has been estimated that SLR at the Dutch coast can reach up to 1.2 m by 2100 compared to the 1995-2004 mean (KNMI, 2021). Therefore, coastal protection and adaptation to the rising sea levels is crucial in the Netherlands.

As the vulnerability of coastal areas increases with climate change, so does the need for adaptation. The Intergovernmental Panel on Climate Change (IPCC) defines adaptation as "the process of adjustment to actual or expected climate change and its effects" (Barros et al., 2014, p. 1758). Here the focus lies on climate adaptation through the implementation of coastal protection measures against SLR. For the 21st century, the benefits of coastal adaptation against SLR were found to outweigh the social and economic costs of inaction (Wong et al., 2014). Two distinct types of coastal adaptation can be distinguished: 'hard' technical measures and 'soft' nature-based solutions.

In the Netherlands, coastal protection focused on 'hard' engineering solutions after the North Sea flood in 1953, such as seawalls, dams, dikes and breakwaters (van Slobbe et al., 2013). A prime example is the Eastern Scheldt storm surge barrier (*Oosterscheldekering*), which is a nine-kilometre-long series of dams and storm surge barriers to protect against flooding from the North Sea. Even though such technical solutions can be highly effective, they are costly to build and maintain, can cause coastal erosion or damage in adjacent areas, can lead to ecological degradation and fail (Chiu et al., 2021; Moraes et al., 2022; Stancheva et al., 2011). Moreover, these structures decrease the natural capacity of coastlines to adapt and need continuous heightening and widening to keep up with SLR (Temmerman et al., 2013). Because of these detrimental effects, the Dutch government applied the national policy of dynamic preservation of the coastline in 1990 (Rijkswaterstaat, 1990), which led to a paradigm shift to also include more 'soft' solutions in Dutch coastline management (Brière et al., 2017).

'Soft' solutions, so called Nature-based Solutions (NbS), take a more natural approach to coastal protection. Here I define coastal NbS as: management options for coastal protection that include elements and processes of coastal ecosystems. Other terms, such as *Building with Nature* and *Ecosystem-based* coastal defence are also used for such measures (de Vriend et al., 2014; Temmerman et al., 2013). Because NbS use natural systems for coastal protection, they leave room for natural adaptation of the coastal system to pressures such as climate change (Hale et al., 2009). This means that, NbS are self-regulative measures that take a proactive approach to coastal protection (de Vriend et al., 2014; Jordan

& Fröhle, 2022). NbS can function as coastal defences by attenuating and dissipating waves, accumulating sediments, and slowing or halting coastal erosion (Jordan & Fröhle, 2022). Apart from coastal protection NbS also other ecosystem services, such as carbon sequestration, space for recreation, water quality improvement and habitat provision(Temmerman et al., 2013). Examples of coastal ecosystems that are used in the Netherlands as coastal NbS are salt marshes, seagrasses and oyster reefs.

Salt marshes are areas vegetated by salt-tolerant plants, which are exposed to periodic flooding due to fluctuating tidal water levels (Adam, 1990; van Loon-Steensma, 2015). Salt marshes form a vegetated transition zone between land and water and have been found to dampen incoming waves to coastlines (Anderson & Smith, 2014; Christie et al., 2018; van Loon-Steensma, 2015). Salt marshes were found to attenuate waves by up to 50% in summer and 10% in winter periods (Schoutens et al., 2019). As waves are dampened, the height of dikes can be decreased and less reinforcements are needed at coasts with salt marshes (Penning et al., 2016). The risk of dike breaching was also found to be lowered when salt marshes are present (Zhu et al., 2020). Furthermore, due to the reduced wave intensity, salt marshes decrease the amount of coastal erosion (Barbier et al., 2011).

Seagrasses are flowering plants that are present in marine environments. Seagrass species have been demonstrated to increase coastal protection through attenuating waves and stabilising sediments in shallow coastal areas (Bos et al., 2007; Ondiviela et al., 2014; van Katwijk et al., 2016). Wave heights were found to be reduced by up to 70% by seagrass vegetation (Hansen & Reidenbach, 2012). By influencing their environment, seagrasses function as ecosystem engineers (Bos et al., 2007). However, it is dependent on the characteristic of the ecosystem how effective seagrasses or salt marsh are in protecting coasts (Twomey et al., 2020, 2022).

Oyster reefs, aggregation of oysters that form colonial communities, have also been found to dissipate waves and reduce coastal erosion (Cheong et al., 2013; Scyphers et al., 2011; Thomas et al., 2022). Oyster reefs act as natural breakwaters in front of coasts and are important ecosystem engineers in intertidal and subtidal coastal areas (Cobacho et al., 2020; Fivash et al., 2021). Oyster reefs were found to attenuate up to 95% of waves, depending on height and width of the reef (Cheong et al., 2013). However, due to overexploitation and the construction of dams, their establishment and survival rate has decreased (Beck et al., 2011; Christianen et al., 2018). Estimates show that globally 85% of oyster reefs have been lost (Beck et al., 2011). Therefore, recently artificial oyster reefs have been constructed, which have an important function as coast stabilisers (Fivash et al., 2021; Walles et al., 2015, 2016). In addition, oyster reefs have the ability to grow with increasing sea-levels both vertically and laterally over time, thereby increasing their climate adaptation capability (Fivash et al., 2021).

The habitats introduced above that function as NbS for coastal protection are all present in the Dutch Wadden Sea. The Wadden Sea is an intertidal coastal landscape, which means that it is an area between high and low tide. The Wadden Sea has been recognised as a unique, ecologically rich and diverse ecosystem with outstanding natural value, and has received the UNESCO World Heritage site status (Hofstede & Stock, 2018; Walsh, 2018). Furthermore, it performs a key function in protecting the land from flooding, due to its vegetation, the barrier islands, and intertidal flats (van Loon-Steensma, 2015). However, as a low-lying and gradually changing coastal area, it is particularly vulnerable to climate change and SLR (Walsh, 2018).

1.2.   Research gap

The recognition and application of NbS for coastal protection has increased, with an increase in the research on these solutions (e.g., Bos et al., 2007; Cobacho et al., 2020; van Loon-Steensma, 2015). When NbS are present in an area, the bed roughness is increased as the NbS create obstacles to the flow (Figure 1). Thereby there is a higher resistance to the flow over the NbS and the flow velocity is reduced. This could consequently decrease the water level that reaches the coast. However, the research on salt marshes, seagrasses and oyster reefs has mainly focused on the wave dissipation effect of these NbS

(e.g., Christie et al., 2018; Pinsky et al., 2013; Salatin et al., 2022; Twomey et al., 2020). However, the effect that these NbS have on the water depth and flow velocity are also important indications for the coastal protection service of NbS. For example, the decreased flow velocity and water level can decrease the bed shear stress and thereby the amount of erosion in an area. All these pathways decrease the amount of hydrodynamic forces that reach the coast and can consequently protect the coast from inundation and erosion (Figure 1).
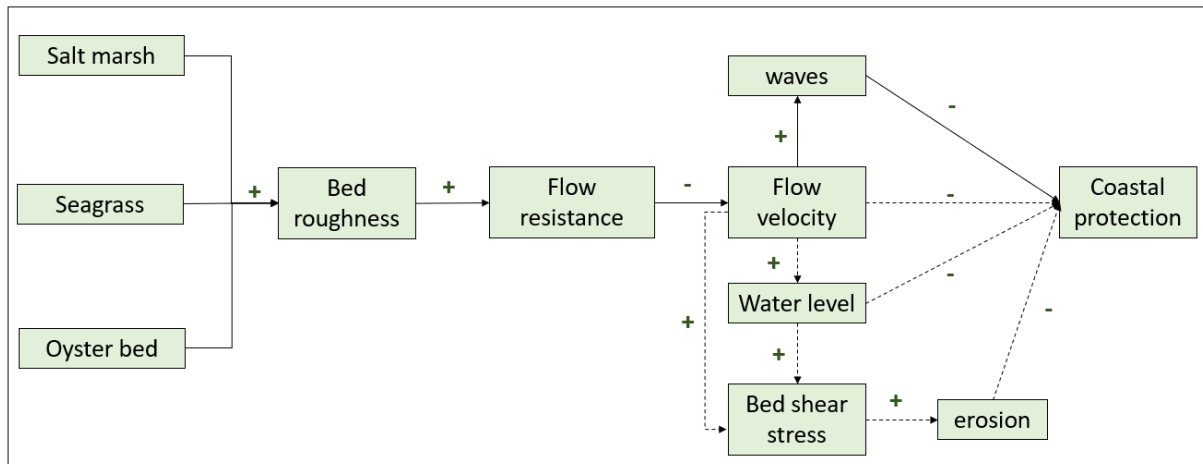
Figure 1. The pathway for how different NbS can influence coastal protection. The dashed lines are studied in this thesis, as these have been understudied compared to wave dissipation effect of NbS.

In addition, a key uncertainty is whether the NbS will protect coasts from future SLR caused by climate change, especially if worst-case climate change scenarios will become reality. Marijnissen et al. (2020) and van Loon-Steensma (2015) found that salt marshes are effective ways for coastal protection with future SLR in the Dutch Wadden Sea. However, the results of Best et al. (2018) predict that salt marshes will initially be resistant and able to adapt to SLR, but after 50-60 years will start to drown and lose their coastal protection function. Therefore, there is an uncertainty in the scientific literature whether coastal ecosystems will be able to protect the coastline with SLR due to future climate change.

The effect of NbS are researched in different locations, which makes the comparison between the effectiveness of NbS alternatives difficult. So far, to my knowledge, no comparison has been made between the effectiveness of salt marshes, seagrasses and oyster reefs in the same setting. As the Uithuizerwad and Groningerwad area, which lie within the Wadden Sea region (Figure 2), are home to all of these habitats, it is an ideal location for the comparison of the different NbS.

1.3. Purpose

The aim of this thesis is to identify how different NbS can help with coastal protection. More specifically, the effect of salt marshes, seagrass meadows and oyster beds are studied, which are important coastal habitats in the Wadden Sea. To understand the effects of these different NbS, an area where all three NbS are present is studied within the Wadden Sea, the Groningerwad and Uithuizerwad area (Figure 2).

The main research question of this thesis is:

To what extent can Nature-based Solutions contribute to coastal protection in the Groningerwad and Uithuizerwad areas in the Dutch Wadden Sea?

This main research question breaks down into the following sub-research questions:

- What is the coastal protection potential of salt marshes, seagrasses, and oyster beds in the Groningerwad and Uithuizerwad areas?

- How does the coastal protection potential of salt marshes, seagrasses and oyster beds differ from each other?
- What is the coastal protection potential of NbS for different SLR scenarios in 2100?
- What parameter defines the coastal protection potential of the NbS?

The coastal protection potential is studied by looking at the difference in the water depth, flow velocity and the degree of erosion. It is expected that the water depth, degree of erosion and flow velocity decrease when NbS are present. This is important, as this would mean that lower hydrodynamic forces reach the coastline in the Groningerwad and Uithuizerwad and that less 'hard'' engineering solutions need to be taken. These three indicators for coastal protection were studied as these were identified to be pathways for NbS to influence coastal protection (Figure 1) and have been understudied compared to the effect on the wave height.

First, in Section 2, the methods that were used for this thesis are described, with a description of the study area, the model setup, the implementation of NbS in the model and the scenario analysis. The sensitivity analysis is also described, which was used to determine the parameter that defines the coastal protection potential of the NbS. In section 3 the results are described to give answers to the research questions. In section 4, these results are discussed, put into context with the findings of other studies and limitations and uncertainties of this thesis are mentioned. Lastly, in section 5, conclusions are drawn from the findings of this thesis and recommendations for further research are made.

2. Methods

2.1. Study area

The study area is located in the Wadden Sea in the Netherlands and includes the Groningerwad and Uithuizerwad intertidal zones (Figure 2). It lies north of the coast of the Groningen province and south of the Schiermonnikoog, Rottumerplaat and Borkum islands and their inlets. It has a size of 34163 ha and has a coastal length of 39 km. Using the Amersfoort RD New coordinate system (EPSG: 28992), the study area has a minimum longitude of 212.44 km and latitude of 601.08 km, and a maximum of 249.73 and 620.11 km. The area is characterised by a wide expanse of mudflats, sandbars and salt marshes that are exposed during low tide and flooded during high tide. Due to these dynamic conditions, the area is home to a rich variety of species, including salt marsh species, seagrasses, and bivalves.

Figure 2. Study area (red) including the Groningerwad and Uithuizerwad. With the locations that were used to observe outputs from the model: observation points with their names (white points) and cross sections (white lines).

One of the most dominant salt marsh species in the Wadden Sea region, including the study area, is *Spartina anglica*, the common cordgrass (Nehring & Hesse, 2008). It was introduced to the Wadden Sea in the early 20th century to stabilise mudflats and prevent erosion (Wolff, 2005). Since then it has outcompeted some native species and has become an important part of the plant community in the Wadden sea (Nehring & Hesse, 2008). It is mostly present at the seaward side of salt marshes, where it forms an almost monotypic belt (Nehring & Hesse, 2008).

The two main seagrass species that are found in the Wadden Sea are *Zostera marina* (eelgrass) and *Zostera noltii* (dwarf eelgrass). Many *Z. marina* beds have disappeared from the Dutch Wadden sea during the last century, for example, a 65-150 km² bed was lost in the 1930s due to a wasting disease (Van Katwijk & Hermus, 2000). Although in smaller bed extents, the species is still present in the Ems-Dollard estuary (de Jonge et al., 2000). Restoration projects are also taking place with, for example, four ha of *Z. marina* sowed in the study area in 2015 (Govers et al., 2018). Most of the seagrass occurring in the Wadden Sea belongs to the perennial species *Z. noltii*. Currently, the total seagrass bed extent in the Dutch Wadden Sea is only 11.3 hectares in total of these two species (Govers et al., 2022). Many attempts to restore seagrass meadows are currently in progress (Van Katwijk et al., 2016).

Ostrea edulis, the European flat oyster, is a native species to the Wadden sea. However, its population went extinct due to overfishing and bottom trawling in the 20th century (Smaal et al., 2015). Since 2015 it has reappeared in the Dutch Wadden Sea (Christianen et al., 2018; Jacobs et al., 2020). Subsequently, reintroduction projects of the species have started (Smaal et al., 2015). Furthermore, the non-native *Crassostrea gigas* (Pacific oyster) is also abundantly present in the Wadden Sea (Jacobs et al., 2020). These two oyster species are often found to co-exist, with the native oyster being attached to the hard shell substrate of the invasive oyster (Christianen et al., 2013).

The above-mentioned species were studied as NbS in the Groningerwad and Uithuizerwad area. The salt marsh was represented by parameters of *S. anglica,* the oyster bed by *O. edulis* and *C. gigas*, and the seagrass fields by *Z. marina* and *Z. noltii*. The impacts on the water regime of these different species were studied in a numerical model.

2.2. Model set-up

2.2.1. Model description

A model developed by Schrijvershof et al. (2023) in the Delft3D Flexible Mesh (FM) model suite was used to study the effect of the different NbS. The Delft3D-FM (v. 2023.01) suite is a process-based, numerical, open-source model developed by Deltares with several modules (Schrijvershof et al., 2023; Vermeersen et al., 2018). Here, the hydrodynamic Flow module (D-Flow) is used to look at the influence of NbS on the hydrodynamics within the study area. As depth-averaged two-dimensional models were found to capture similar and reliable results in tidal basins as three-dimensional models (Horstman et al., 2015; Lokhorst et al., 2018), a two-dimensional model was used.

As the model extent the whole Ems-Dollard estuary was studied (Figure 3), rather than only the Uithuizerwad and Groningerwad area. By modelling the whole Ems-Dollard estuary, hydrodynamic processes present at a larger scale than the Groningerwad and Uithuizerwad could be taken into account. The estuary includes the Ems river (from the Ems-Dollard estuary up to an 86 km upstream weir), the intertidal zone of the Wadden Sea in front of the Ems-Dollard estuary (from the Schiermonnikoog to the Norderney islands), and a 32 km strip of the North sea in front of these islands (Figure 3). The model area has a size of 5557 ha, and a minimum longitude of 176.46 km and latitude of 562.04 km, and a maximum of 295.20 and 665.64 km.

Figure 3. The modelled Ems-Dollard estuary (red) and the study area (black) with the initial bathymetry (m compared to NAP).

The D-Flow module of the Delft3D-FM model was used to model the hydrodynamic conditions in the Ems-Dollard estuary (Deltares, 2022). This numerical hydrodynamic modelling system computes non-steady flow and transport processes that are a result of tidal and meteorological forcings (Deltares, 2022). Three main depth-averaged unsteady shallow water equations are used within this model: (1) the continuity equation, (2) the horizontal equation of motion (momentum equation), and (3) the transport equation of conservative constituents (vertical velocity). These equations are described in Appendix C. By using these equations, the following assumptions are made in the hydrodynamic model: mass conservation within the system, shallow water conditions (vertical depth assumed to be much smaller than the horizontal scale of depth), and the Boussinesq assumption (vertical variation in the fluid velocity assumed to be much smaller than the horizontal velocity).

Within the water equations the flow velocity, water level and bed shear stress are described, which were used as measures for the coastal protection within this study. For the flow velocity the magnitude of the depth-averaged velocity (/U/) variable was studied (m s^{-1}), which is calculated by:

$$|U| = \sqrt{u^2 + v^2} \qquad\qquad Eq.\ 1$$

u and v are the horizontal depth averaged flow velocities (m s^{-1}) in x- and y-directions. The bed shear stress (τ; Pa) is described by the quadratic friction law (Deltares, 2022):

$$\tau = \frac{p_0 g U |U|}{C_{2D}^2} \qquad\qquad Eq.\ 2$$

Where P_0 is the initial density (kg m^{-3}), g is the gravitational acceleration (m³ kg^{-1}) and U is the depth-averaged velocity (m s^{-1}). C_{2D} is the roughness coefficient, which was calculated by the Manning formulation (Manning, 1891) for this research:

$$C_{2D} = \frac{\sqrt[6]{R}}{n_m} \qquad\qquad Eq.\ 3$$

Where R is the hydraulic radius, which is in case of the here applied depth-averaged model the water depth, and n_m the Manning's roughness value (m$^{1/3}$ s^{-1}).

2.2.2. Boundary and initial conditions

Different boundary and initial conditions were used in the model of Schrijvershof et al. (2023). Here the grid, bathymetry, bed roughness and water level are described. Additionally, the timeframe of the model and the observation points and cross sections that were used for the model outputs are introduced.

Grids of varying density were used in the model (Figure A 1). The offshore area has a large grid size (up to 1 km) with grids becoming progressively smaller towards the study area and the upward part of the river Ems (up to 30 m). In the study area the grids have a size around 300 m. By using grids of varying sizes, smaller scale processes could be considered more accurately in the river and study area, while computational time did not have to increase significantly. The flexible mesh property of the Delft3D-FM model made this variability in grids possible.

An initial bathymetry was prescribed to the model (Figure 3). This bathymetry was based on echosounding observations from 2014 in the area (van Prooijen et al., 2020). These observations have been made publicly accessible by the Dutch Directorate-General for Public Works and Water Management (Rijkswaterstaat, n.d.). The initial bathymetry for the model was set up by Schrijvershof et al. (2023).

A spatially varying initial bed roughness was used for the Ems-Dollard estuary. The Manning's roughness value was used as a measure for the roughness of the bed, with higher values indicating rougher and lower values smoother beds. The roughness varied between a Manning's roughness value of 0.019 m$^{1/3}$ s^{-1} at the sea and the mouth of the river, to 0.011 m$^{1/3}$ s^{-1} at the upstream end of the river. A smoother bed roughness was set up in the river bed by Schrijvershof et al. (2023) in order to prevent

overestimation of the dampening of the tide of the Ems river (Schrijvershof et al., 2023). This spatially variable bed roughness was applied for this study as well to prevent this overestimation.

Water level boundary conditions were used for the open boundaries of the model area. Open boundaries are present at the seaward side and the upper sections of the rivers, while impermeable boundaries are present at the coasts and riverbanks of the model. For the water levels at the seaward side, outputs from the North-Western European Shelf hydrodynamic model (3D DCSM-FM) developed by Zijl et al. (2021) were used from 2018 to 2019. For the upstream end of the Ems river a time-varying river discharge derived from observations was used (varying between 30-300 m³ s⁻¹; Schrijvershof et al., 2023). For three other locations where small rivers flow into the Ems river, river discharges were used: Delfzijl (Old Ems channel), Leer (Leda) and Nieuwe Statenzijl (Westerwoldse Aa).

The model was run for a time period of 127 days from the 25th of December 2018 till the 1st of May 2019 (Figure 4). The 1st of January 2000 was used as a reference date, which is an arbitrary t=0 point for all the time series used and simulated by the model (Deltares, 2022). This means that all the output files are specified as seconds after this reference time. The user time step was set to five minutes, which is the interval with which the meteorological forcings are updated, as well as the computational time step that is used in the model (Deltares, 2022). A nodal time step of six minutes was used for the astronomic boundary conditions. For the time series output data from the model a time step of one hour, while for the map output data one day was used. For the outputs, a one-week period at the beginning of the simulation is excluded from the analysis in order for the modelled system to arrive at hydrological equilibrium conditions.
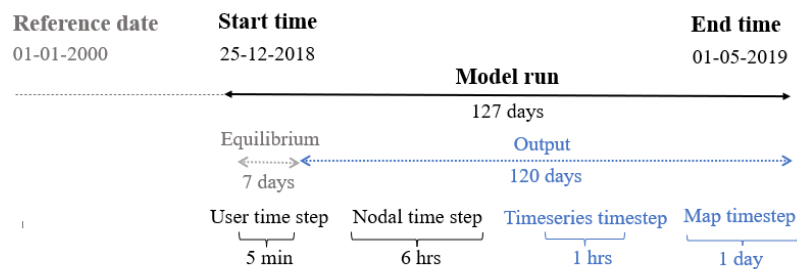
Figure 4. Timeframe and timesteps used in the model.

Different observation points and cross sections were added to the model (Figure 2), which are the locations for which model outputs were generated. Two observation points were added to the Groningerwad and Uithuizerwad coast, as well as to a transect along the intertidal zone. One cross section was added along the coast and three parallel to the coast along the study area. At the observation points the water depth and bed shear stress were studied, while at the cross sections the flow velocity was observed.

2.3. Implementation of NbS

The effects of the NbS were implemented in the model through parameterising their characteristics and quantifying the shear stress that they exert on the passing flow. Thereby a relationship between the presence and the spatial distribution of the NbS on the flow resistance could be considered. The shear stress that the NbS have on the flow was calculated by the method of Baptist et al. (2007; section 2.3.1). The flow resistance exerted by the NbS was resolved in the D-Flow module by applying the trachytope functionality (section 2.3.2; Deltares, 2022).

2.3.1. Baptist method

The Baptist et al. (2007) method calculates the resistance that vegetation exerts on the flow. The equations of Baptist et al. (2007) combine the resistance on the flow inside the vegetation with the logarithmic profile above the vegetation (Baptist et al., 2007). Thereby they consider the flow through

and over the NbS and can be used for both submerged and non-submerged conditions (Baptist et al., 2007; Deltares, 2022). The equations use an analytical solution for the resistance induced by NbS in the momentum balance (Deltares, 2022). This includes the water depth dependency, which makes the two-dimensional depth-averaged modelling of the three-dimensional NbS possible. The equations proposed by Baptist et al. (2007) represent NbS as rigid cylinders which exert resistance on the flow (van Leeuwen, 2008). Because of this, the NbS can be represented by three parameters: the height of the NbS (h_v), the density of the NbS (n) and the drag coefficient (C_d) (for the list of variables with units see Table B 1).

With the NbS parameters, a representative bed roughness (C), the so called Baptist roughness predictor, is calculated with the following equation for when the NbS are submerged (Baptist, 2005; Deltares, 2022):

$$C = C_b + \frac{\sqrt{g}}{\kappa} \ln \frac{h}{h_v} \sqrt{1 + \frac{C_D n h_v C_b^2}{2g}}$$

Eq. 4

With C_b being the bed roughness (Chèzy roughness) without NbS present (m$^{0.5}$ s^{-1}), κ the Von Kármán constant (-), h the water depth (m) and h_v the height of the NbS (m). The C_b value is calculated with:

$$C_b = 18 \log(12h/D_{90})$$

Eq. 5

Where D_{90} is the 90th percentile of the grain size, meaning that 90% of the sediment in the area is smaller than this value. For the study area a grain size of 500 μm and a typical depth of 5 m was used (Barua, 2020; Reef et al., 2018). These conditions are typically found in tidal basins and are also present in the Wadden Sea region (Best, 2017; Zeiler et al., 2014). With these values a C_b value of 83 m$^{0.5}$ s^{-1} was calculated.

The representative bed roughness consequently affects the flow resistance (λ) of the NbS in the submerged conditions:

$$\lambda = C_D n \frac{h_v C_b^2}{h C^2}$$

Eq. 6

In case of non-submerged NbS, which means that $h<h_v$, the flow resistance and bed roughness can be separated (Eq. 7-8).

$$C = C_b \qquad\qquad\qquad \textit{Eq. 7}$$

$$\lambda = C_D n \qquad\qquad\qquad \textit{Eq. 8}$$

The effect of the NbS on the hydrodynamics is thereby parameterised in a bed roughness, which consequently affects the bed shear stress. The representative bed roughness is incorporated in the flow momentum equation (Eq. 22-23) through the following loss term due to bed friction (van Leeuwen, 2008):

$$-\frac{g\,U\,u}{C^2 h} \qquad\qquad\qquad \textit{Eq. 9}$$

Where u is the depth averaged velocity (m s^{-1}) and U is the absolute magnitude of velocity (m s^{-1}; Eq. 1). Furthermore, the flow resistance of the NbS is subsequently included as a sink term in the momentum equation (Eq. 22-23; Deltares, 2022; Van Veelen et al., 2010):

$$-\frac{\lambda}{2}u^2 \qquad\qquad\qquad \textit{Eq. 10}$$

By including the flow resistance exerted by the NbS and not only the bed roughness, it is prevented that an increased bed roughness automatically leads to an excessively high bed shear stress and large sediment transport rate (Deltares, 2022). Other methods do make this overestimation in the bed shear stress (e.g. Klopstra et al., 1996).

2.3.2. Trachytope functionality

The Baptist et al. (2007) equations were implemented in the model through the trachytope functionality of the Delft3D-FM model. This functionality allows the specification of the bed roughness and flow resistance on a sub-grid level by the use of land use or roughness/resistance classes (Deltares, 2022). The term trachytope comes from the Greek word τραχυτης, which means roughness (Deltares, 2022).

The trachytopes were included in the model through a trachytope definition file (.ttd file) and a spatial distribution file (.arl file). The definition file includes the parameters h_v, n and C_d per NbS, to which a trachytope number is added. The method, in this case Baptist et al. (2007), and C_b value are also specified in this file. The spatial distribution file contains: (1) coordinates of the flow links, which are midpoints of the netlink that connects two flow nodes, (2) trachytope numbers, and (3) an area fraction of the NbS (f_i) to determine the distribution of the NbS within the model area. Thereby the trachytope number connects the distribution with the definition file. When the fraction is less than one, the background roughness is used, which has a Manning's value of 0.019 $m^{1/3}$ s^{-1}. The trachytopes were converted in the model into the representative bed roughness (C) and the linear flow resistance coefficient (λ) per velocity point (index j) with an update interval of 10 minutes. The C and λ values were accumulated proportionally to the surface area fraction (f_i) as defined in the spatial distribution file (Eq. 12-13).

$$C_{area} = \sum_i f_i C_i$$

Eq. 11

$$\lambda = \sum_i f_i \lambda_i$$

Eq. 12

The total bed roughness of the area was then calculated by accumulating the inverse of the squared Chèzy value (Eq. 14)

$$\frac{1}{C_{total}^2} = \frac{1}{C_{area}^2}$$

Eq. 13

Because of the relatively short time of simulation (five months), the impacts that the hydrodynamics have on the growth and mortality of the NbS are not considered in the model.

2.3.3. NbS parameterisation

The different NbS were represented in the model using the parameters h_v, n and C_d (Eq. 4-11;Table 1). The NbS had to be parameterised because the vegetation and oysters are smaller than the model grid and therefore not explicitly solved on the grid level. The parameters for the NbS were defined by using data from earlier studies, which will be introduced in the following paragraphs. The studies were selected to have similar habitat and environmental conditions as in the study area when possible. By representing the NbS by these parameters several assumptions were made: (1) uniform height of the NbS within the canopy, (2) uniform density, and (3) a constant drag coefficient per NbS.

Table 1. The different parameters for the NbS indicated with the sources from which they were found.

Species	Parameter		Value	Unit	Source
Zostera noltii	vegetation height	h_v	0.3	m	(Familkhalili & Tahvildari, 2022; Valle, 2014)
	shoot density	p	3669.5	m^{-2}	(Polte et al., 2005; Schanz & Asmus, 2003; Valle, 2014; Zipperle et al., 2009)
	leaves per shoot	m	3	[-]	(Schanz & Asmus, 2003)
	leaf width	D	0.002	m	(Borum et al., 2004; Luhar et al., 2010)
	n (density)	n	22.017	m^{-1}	
	drag coefficient	C_d	1.54	[-]	(Familkhalili & Tahvildari, 2022; Ondiviela et al., 2014; Paul & Amos, 2011; Twomey et al., 2020)
Zostera marina	vegetation height	h_v	0.45	m	(Borum et al., 2004; Bostrom & Bonsdorff, 2000; Laugier et al., 1999)
	shoot density	p	1451.37	m^{-2}	(Borum et al., 2004; Bostrom & Bonsdorff, 2000)
	leaves per shoot	m	5	[-]	(Laugier et al., 1999)
	leaf width	D	0.005	m	(Bostrom & Bonsdorff, 2000; Jacobs et al., 2008; Nienhuis & De bree, 1980; Olesen & Sand-Jensen, 1994)
	n (density)	n	36.28	m^{-1}	
	drag coefficient	C_d	0.755	[-]	(Follett et al., 2019)
Spartina anglica	vegetation height	h_v	0.5	m	(Basismonitoringwadden, 2020)
	shoot density	p	1190	m^{-2}	(Vuik et al., 2018)
	leaves per shoot	m	7	[-]	
	stem diameter	D	0.0035	m	(Vuik et al., 2018)
	density	n	29.155	m^{-1}	
	drag coefficient	C_d	0.7	[-]	(Willemsen et al., 2022)
Oyster bed	oyster bed height	h_v	0.0495	m	
	number of oysters	p	230	m^{-2}	
	oyster diameter	D	0.066	m	(Christianen et al., 2018)
	density	n	15.18	m^{-1}	
	drag coefficient	C_d	0.031	[-]	(Kitsikoudis et al., 2020)
	bed level change		0.05	m	(Walles et al., 2015)

The vegetation height of the *Z. noltii* seagrass species was set to 0.3 m, based on the value calculated for a modelling study (Familkhalili & Tahvildari, 2022). For the *Z. marina* species a vegetation height of 0.45 m was used, based on measured leaf lengths (Borum et al., 2004; Bostrom & Bonsdorff, 2000) and a deflected leaf height (Laugier et al., 1999). The density was calculated with the following equation:

$$n = pmD \qquad \text{Eq. 14}$$

Where p is the shoot density (shoots m^{-2}), m is the number of leaves per shoot and D is the leaf width (m). The shoot density for *Z. noltii* and *Z. marina* were calculated from a range of values measured in different studies (Table 2). The average shoot density value for *Z. noltii* was found to be 3669.5 shoots m^{-2} and for *Z. marina* 1451.37 shoots m^{-2}. The number of leaves per shoot for *Z. noltii* was found to be three and for *Z. marina* five (Laugier et al., 1999; Schanz & Asmus, 2003). The leaf width was found to be two and five mm for *Z. noltii* and *Z. marina* respectively (Borum et al., 2004; Bostrom & Bonsdorff, 2000; Luhar et al., 2010). From these values an *n* value of 22.02 and 36.28 m^{-1} was calculated for the *Z. noltii* and *Z. marina* species (Table 1).

Table 2. The shoot density of the Z. marina and Z. noltii species as calculated by different studies. With the mean, minimum and maximum density indicated.

| Species | Shoot density | | | Source |
	mean	min	max	
Z. noltii	3500	2000	5000	Schanz & Asmus, 2003
	6544	1088	12000	Polte et al., 2005
	1634	426	2842	Zipperle et al., 2009
	3000	4000	2000	Valle, 2014
Z. marina	1480	390	2570	Jacobs et al., 2008
	2125.5	651	3600	Olesen & Sand-Jensen, 1994
	1950	300	3600	Nienhuis & De bree, 1980
	250	50	500	Bostrom & Bonsdorff, 2000

A C_d value of 1.54 for the *Z. noltii* species was calculated from an average of a range of studies shown in Table 3. For *Z. marina* a non-rigid blade C_d value of 0.755 was used, based on a range calculated by Follett et al. (2019).

Table 3. The drag coefficient of the Z. noltii species as defined by different studies.

C_d	Source
1.58	Familkhalili & Tahvildari, 2022
1.1	Twomey et al., 2020
1.8	Maza et al., 2012
1.67	Paul & Amos, 2011

The height of the salt marsh vegetation (0.5 m) was determined by measurements of the vegetation in different plots measured by a Dutch salt marsh organisation (Basismonitoringwadden, 2020). For the shoot density a maximum stem density for the *S. anglica* species of 1190 stems per m² was used, which was calculated by Vuik et al. (2018) in the Western Scheldt estuary. The stem diameter was set to 3.5 mm (Vuik et al., 2018). With an assumed seven stems per plant, the *n* parameter for the salt marsh vegetation was calculated to be 29.15 m^{-1}. For the C_d a value of 0.7 was used, which takes into account different conditions and vegetation ages of the *S. anglica* species (Willemsen et al., 2022).

The *n* parameter of the oyster reef was calculated from the oyster diameter and the number of oysters per m². An oyster diameter of 6.6 cm was used, based on the average of shell widths of *O. edulis* measured at the North Sea coast in the Netherlands (Christianen et al., 2018). It was assumed that oysters occupy the whole bed where they are present. So, the density was calculated with the diameter, and found to be 230 oysters m^{-2}. From these values an *n* parameter of 15.18 m^{-1} was calculated. The h_v of the oyster bed was assumed to be 1.5 times the thickness of an *O. edulis* oyster, and was therefore set to 0.0495 m. From the literature, no C_d value was found for either the *O. edulis* or the *C. gigas* species. Therefore, a C_d of the *C. virginica* oyster species was used, which was found to be 0.031 (Kitsikoudis et al., 2020). Furthermore, because sedimentation takes place in oyster reefs, the bed level was increased by 0.05 m. This is based on elevation measurements of *C. gigas* reefs compared to reference areas in the Eastern Scheldt estuary (Walles et al., 2015). The bed level was changed in the model through increasing the values of the initial bathymetry in the study area.

2.3.4. Model runs

The model was first run separately for the different NbS. The NbS were assumed to be present in the whole study area, due to which a density factor of one was used for the study area and zero outside of the study area. However, different density fractions (*n*) as defined during the parameterisation were used in the definition file. The definition files that were used for the models are shown in Table 4.

Table 4. The parameters used in the definition files (ttd.) for the NbS in the trachytope functionality

	Trachytope number	Method number	h_v	n	C_d	C_b
S. anglica	1	154	0.5	29.155	0.7	83
Z. noltii	2	154	0.3	22.017	1.54	83
Z. marina	3	154	0.45	36.28	0.755	83
O. edulis	4	154	0.0495	15.18	0.031	83

Subsequently, a model with a combination of NbS present in the study area was run. Different distributions were used for the NbS (Figure 5) and the assumption was made that the whole study area is covered by NbS. The distribution was based on the current as well as potential extent of the different NbS. For the salt marsh the distribution from a data collection of Wadden Sea maps (Waddenviewer) was used (Basismonitoringwadden, 2020), as well as a map of the distribution in 2004 (Dijkema et al., 2013). For the seagrass distribution the same maps as well as a map for their potential distribution was used (Basismonitoringwadden, 2020; de Jong et al., 2005; Dijkema et al., 2013). For the oyster beds a map with areas of high potential for *O. edulis* occurrence and the current occurrence of *C. gigas* oysters was used to determine their potential distribution in the study area (Didderen et al., 2022). The same parameters were used for the NbS as in the separate runs (Table 4). However, for the seagrass beds it was assumed that the two species showed a 0.5 and 0.5 fraction. The bed level was increased by 0.05 m where the oyster beds were present in the study area.

Figure 5. Distribution of the different NbS used for the combined model run and scenarios.

2.4. Scenarios

The future hydrodynamic conditions in the Wadden Sea depends on two main factors: the relative SLR and the sedimentation in the basin (Vermeersen et al., 2018). Furthermore, the vertical movement of the basin, due to natural processes and anthropogenic activities such as mining and gas extraction, also influence the future dynamics of the system (Fokker et al., 2018). Therefore, scenarios were implemented until 2100, to investigate the response of the system to the changes in SLR, sedimentation and subsidence in the basin. Furthermore, the effect of NbS on coastal protection was studied in these changed hydrodynamic conditions.

2.4.1. Sea level rise

For the SLR three Representative Concentration Pathway (RCP) scenarios were used: RCP8.5, RCP4.5 and RCP2.6. Projections for the Wadden Sea region from Vermeersen et al. (2018) were used for the SLR scenarios. In these scenarios projections are made for the relative SLR, which is the change in the difference between the ocean surface and the ocean floor (Vermeersen et al., 2018). The scenarios are based on the IPCC AR5 climate change projections (Church et al., 2013), and are also compared to

updates derived from more recent literature (Vermeersen et al., 2018). Regional projections (Cannaby et al., 2016) and records (e.g. paleo-records and tide-gauge observations) from the Wadden Sea region are incorporated in the scenario projections (Vermeersen et al., 2018). The total projected change in SLR between 2018 and 2100 is shown in Table 5.

Table 5. Sea level rise (m) in the Wadden Sea region by 2100 from Vermeersen et al. (2018) for the different RCP climate change scenarios. The average for the whole Wadden Sea region is shown with a 5-95% uncertainty range.

Scenario	Sea level rise (m)	Uncertainty (5-95%)
RCP2.6	0.41	0.25
RCP4.5	0.52	0.27
RCP8.5	0.76	0.36

The SLR scenarios were implemented in the model through changing the boundary conditions. The open boundary conditions at the seaward side of the model were increased for different model runs with the amount of SLR projected by the three RCP scenarios. Because the incoming river discharges are very small compared to the tidal prism in the Ems-Dollard estuary (Schrijvershof et al., 2023), no change in the river discharge was applied.

2.4.2. Sedimentation

Changes in sedimentation were not considered in the SLR scenarios, and were therefore separately incorporated into the model. Wang et al. (2018) found that the long-term averaged sedimentation rate in the Dutch Wadden Sea area is 4.5 mm yr^{-1} (Wang et al., 2018). This rate was calculated from observations between 1926 and 2015 in the Wadden Sea region (Wang et al., 2018). This sedimentation rate was extrapolated for this study from 2018 to 2100 (Figure 6), to determine the total sedimentation in the area during this period. The total sedimentation between 2018 and 2100 was found to be 0.37 m.
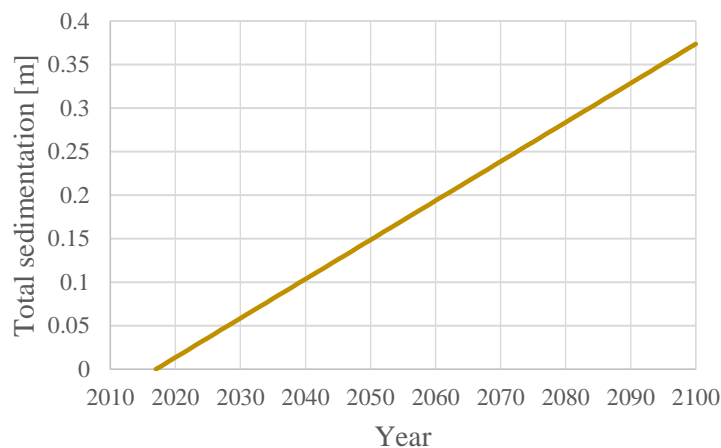
Figure 6. Linearly extrapolated total sedimentation (m) for the Wadden Sea region from 2018 to 2100 based on a sedimentation rate calculated by Wang et al., (2018).

The sedimentation was implemented in the model through changing the initial bathymetry. The bathymetry file, which was used as an initial condition in the model run in 2020, was increased by 0.3735 m in the study area. For the 2100 model, a spatially homogeneous sedimentation was assumed in the study area.

2.4.3. Subsidence

Another process influencing the Wadden Sea region is the vertical movement of the basin due to natural and anthropogenic processes. The three main natural processes that result in a vertical movement of the region are compaction, postglacial isostasy and plate tectonics (Fokker et al., 2018; Kooi et al., 1998). These natural processes act on timescales of thousands of years. For example, for the Ems-Dollard estuary it was estimated that in the 20th century a natural subsidence of less than 0.1 mm yr^{-1} took place in the area (Kooi et al., 1998). Human induced subsidence in the Wadden Sea region is mainly caused

by gas production and salt mining (Fokker et al., 2018). In the study area salt mining is not a relevant contributor to subsidence (Fokker et al., 2018). However, due to gas production the average subsidence rate in the Ems-Dollard tidal basin was found to be 1 mm yr^{-1} with an uncertainty of ± 0.5 mm in 2018 (Fokker et al., 2018; NAM, 2016). Furthermore, projections from 2018 to 2030 indicate an average subsidence of 14 ± 7 mm (Fokker et al., 2018). From 2018 until 2050 the average subsidence is estimated to be 40 ± 20 mm (Fokker et al., 2018). Based on these estimations, the overall average subsidence from 2018 projected until 2100 was estimated to be 101.5 ± 50.75 mm (Figure 7).
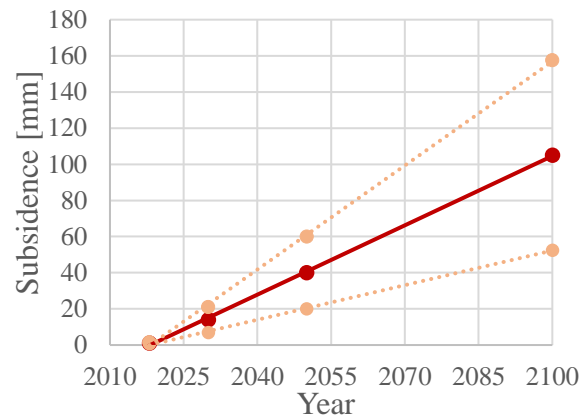
Figure 7. Average subsidence projections of the Ems-Dollard tidal basin from 2018 to 2100 (red) with confidence intervals (orange) extrapolated from estimates by Fokker et al. (2018).

The subsidence of the basin was implemented in the model through changing the bathymetry file of the model run in 2100. The total amount of subsidence used for the study area is 0.10 m. As the amount of subsidence was based on averages for the whole basin, a spatially homogeneous subsidence was assumed. Combining the effects of the sedimentation and subsidence, the initial bathymetry of the Ems-Dollard estuary was increased by 0.26 m.

2.4.4. NbS in the scenarios

To the different SLR scenarios NbS were added in the study area. This was done to determine the effect of the NbS on the coastal protection potential with changed hydrodynamic conditions due to SLR. A combination of NbS, as used for the model run in 2018, was used for the SLR scenarios (section 2.3.4). For this, the same distribution and fraction was used as for the combined model run (Figure 5). Thereby it was assumed that the distribution of NbS did not change over time. In the oyster beds the bed level was not increased as was done in the 2018 model, as a high level of sedimentation was already considered in the scenarios.

2.5. Sensitivity analysis

A sensitivity analysis was performed to determine how the parameters that are used in the trachytope functionality to represent the NbS determine their coastal protection potential. Different values for the h_v, n, C_d and C_b parameters were used while keeping the other parameters constant (Table B 2). These runs were then compared with a reference model run. For the h_v value a range of 0.25 to 1 m was used with 0.25 m intervals, as it is unrealistic for the studied NbS to reach heights above 1 m. For the density value (n) a range from 1 to 1000 was used, to also look at how extremely low and high densities can influence the coastal protection potential of NbS. For the C_d parameter a range between 0.5 and 2 was used, as C_d parameters from other studies were found to range between these values for the NbS (Follett et al., 2019). For the C_b parameter a range between one to 90 m$^{0.5}$ s^{-1} with 30 m$^{0.5}$ s^{-1} intervals was used to find how the background roughness influences the coastal protection potential of NbS. The sensitivity analysis models were run for a shorter time period, for 17 days from the 25th of December 2018 until the 10th of January 2019.

3. Results

3.1. NbS and flow velocity

A lower peak flow velocity was found for the different NbS compared to the reference model with no NbS present. At the coast of the study area, when looking at the daily trend of the flow velocity on the 30th of April 2019, lower amplitudes were found for the seagrass and salt marsh species, while the oyster bed showed a similar trend to the reference model (Figure 8). Further from the coast of the study area similar velocity trends were found for all the NbS, but with lower amplitudes than the reference model.
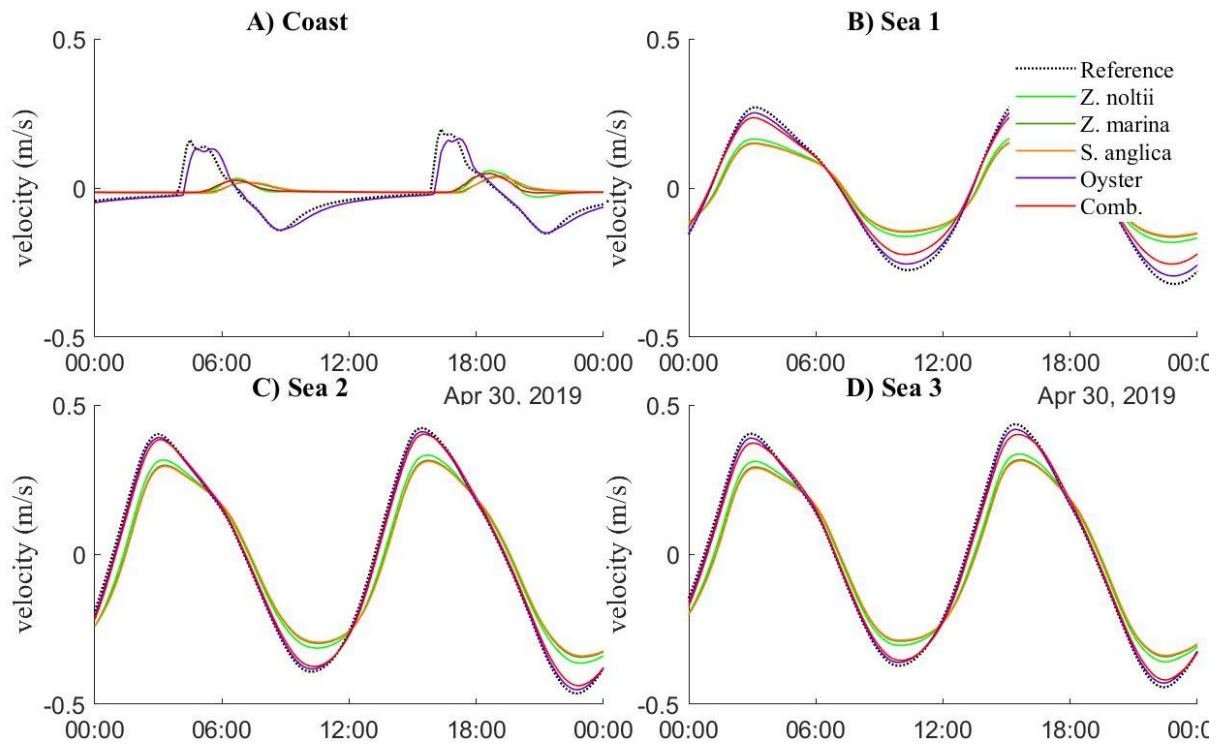
Figure 8. Flow velocity (m s^{-1}) for the different NbS at the cross sections on the 30th of April 2019. Sea 1 is the closest and Sea 3 is the furthest away from the coast (Figure 2).

When looking at the daily maximum velocity over the whole study period lower velocities were found for the NbS (Figure 9). The reference model showed an average daily peak velocity of 0.24 m s^{-1} (SD: 0.04) at the coast from January till May 2019 (Table 6). The oyster bed had the highest peak velocity average (0.21 m s^{-1}, SD: 0.038) of the NbS, while the Z. noltii seagrass bed had the lowest (0.06 m s^{-1}, SD: 0.02). The Z. marina, S. anglica and combined model run had similar mean peak velocity values as the Z. noltii species (Figure 9). The seagrass and salt marsh species showed a decline of about 70% in the peak flow velocity, while the oyster reef showed a decline of 12.5%. For the cross sections at the sea similar results were found, only here the combined model had closer peak values to the oyster bed than the other NbS species (Figure 9).

Table 6. Average peak velocity (m s^{-1}) for the different model runs at the cross sections from January to May 2019. The standard deviations are shown in Table B 3.

	Reference	S. anglica	Z. marina	Z. noltii	Oyster	Combined
Coast	0.237	0.079	0.064	0.063	0.210	0.072
Sea 1	0.337	0.195	0.176	0.172	0.310	0.287
Sea 2	0.503	0.381	0.358	0.353	0.485	0.475
Sea 3	0.528	0.394	0.370	0.364	0.504	0.482
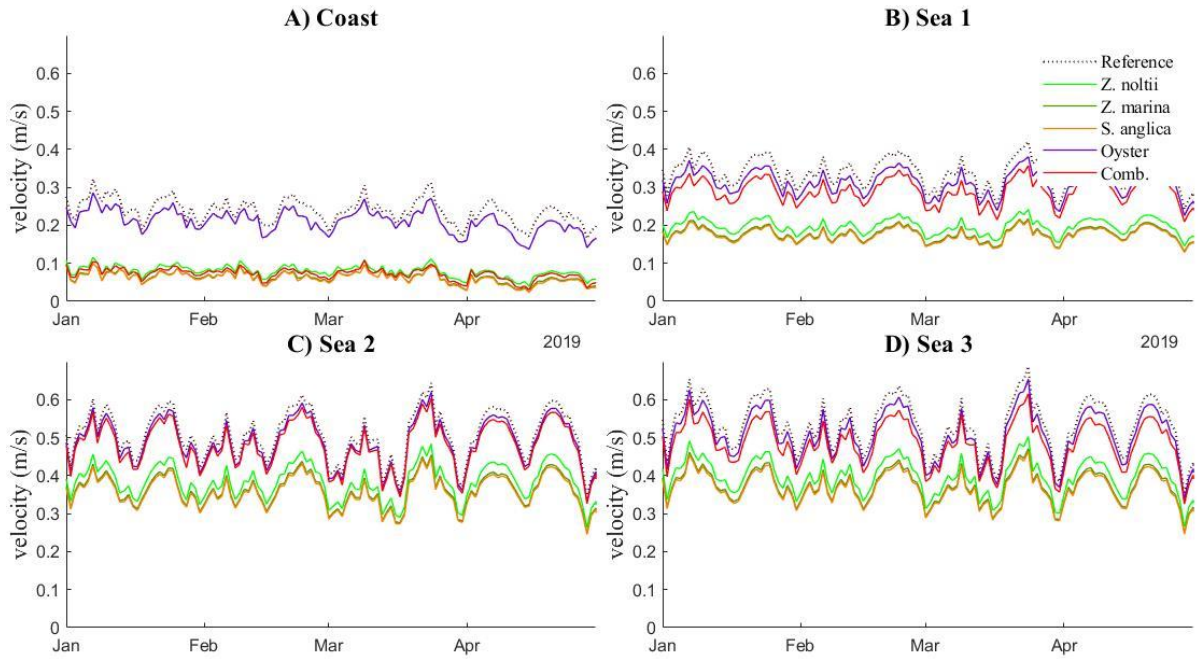
Figure 9. Daily peak velocity at the cross sections over the model period for the different NbS.

3.2. NbS and water depth

The water depth changed when NbS were present in the study area. When looking at the daily trend of the water depth on the 26th of April (Figure 10), the water depth increased during the high tide and decreased during the low tide. The high tide peak water depth value was lower for the NbS than the reference model. At the coast it is dependent on location which NbS shows a lower peak water depth value. At the Uithuizerwad 1 observation point the combination of NbS showed the highest peak values, while the salt marsh species showed the lowest peak values (Figure 10). At the other coastal locations, the oyster bed showed the highest peak value and the *S. anglica* the lowest. Not only the maximum water depth, but also the minimum water depth changed when NbS were present. The duration of dry periods at the coast decreased for the NbS compared to the reference model, except for the oyster bed (Figure 10).
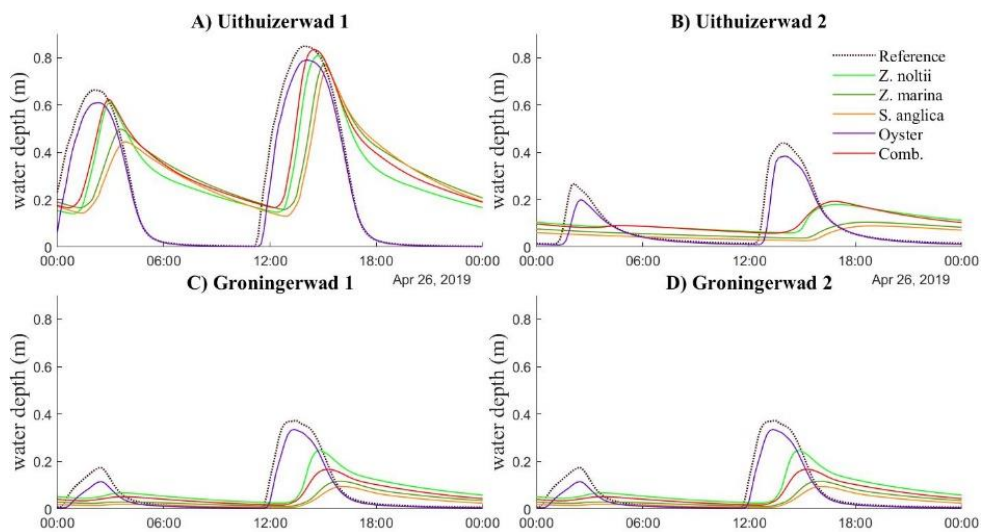
Figure 10. Water depth (m) for the NbS at the coastal observation points in the Uithuizerwad (A-B) and Groningerwad (C-D) for the 26th of April 2019.

When looking at locations further from the coast (Figure 11), lower peak water depth values were observed for the NbS compared to the reference model. Furthermore, the minimum water depth values

at low tide did not reach zero for the seagrass and salt marsh species at the location furthest from the coast in the study area (Figure 11).This means that the intertidal zone remains flooded for a longer period of time. On the other hand, for the combination and oyster reefs dry periods were present, but for a shorter period than the reference model (Figure 11).
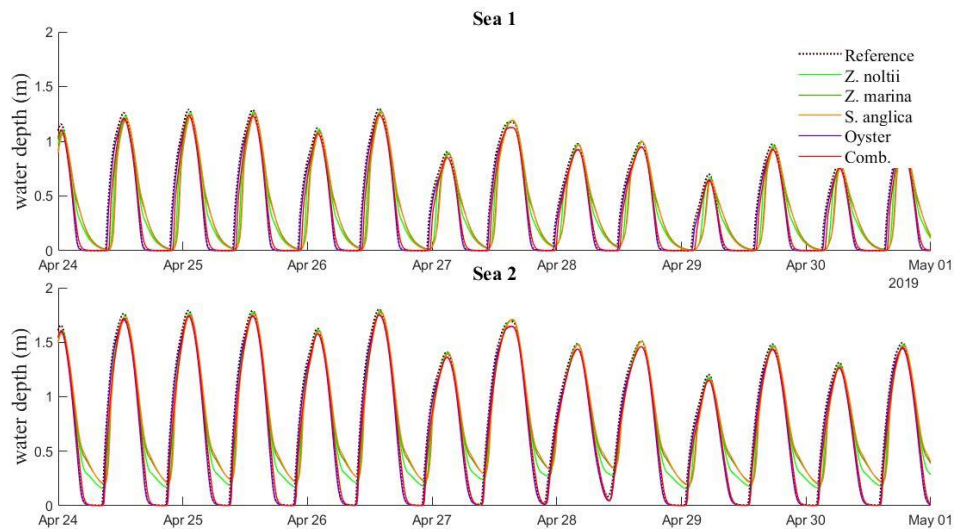
Figure 11. Water depth (m) for the different NbS at the observation points in the Wadden Sea from the 24th of April till the 1st of May 2019.

Because higher peak values and lower minimum values were found for the daily trend of the water depth, these values were studied over the whole study period (Figure 12). Over the whole study period the reference model had an average daily peak water depth value of 1.05 m (SD: 0.37) in the Uithuizerwad and 0.59 m (SD: 0.35) in the Groningerwad (Table B 4). In the Uithuizerwad from the different model runs the combination of NbS had the highest mean peak water depth value (1.02 m, SD: 0.4), while *Z. noltii* had the lowest average peak water depth value (0.91 m, SD: 0.45). For the Groningerwad, the oyster bed resulted in the highest peak water depth value (0.55 m, SD: 0.35) and the *Z. noltii* seagrass bed in the lowest (0.4 m, SD: 0.43). Furthermore, the difference in the peak values of the NbS compared to the reference model were dependent on the magnitude of the peak value. At peaks higher than 1.5 m there was a slight to no difference between the NbS and reference model, while at peaks lower than one metre NbS had lower peak values (Figure 12).
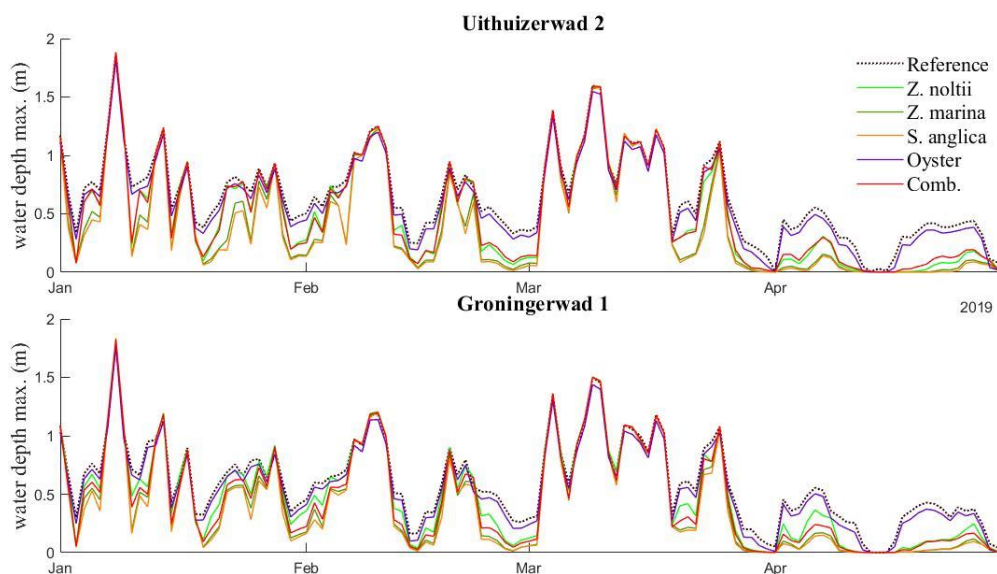
Figure 12. Daily maximum water depth (m) for the NbS at the Uithuizerwad and Groningerwad coast from January to May 2019.

The reference model had an average daily minimum water depth value of zero at the coastline in the study area (Figure 13; Table B 5). The oyster reef showed this same trend. However, the other NbS resulted in a higher minimum water depth over the studied period (Figure 13). At the Uithuizerwad the combined model had the highest daily average minimum water depth (0.16 m, SD: 0.05), while at the Groningerwad the salt marsh species had the highest (0.05, SD: 0.05; Table B 5). Further from the coastline dry periods were present for the reference, oyster bed and combined model (Figure A 2). However, at the location furthest from the coast in the study area no dry periods were present for the seagrass and salt marsh species (Figure A 2), and therefore the study area remained inundated during the whole study period.
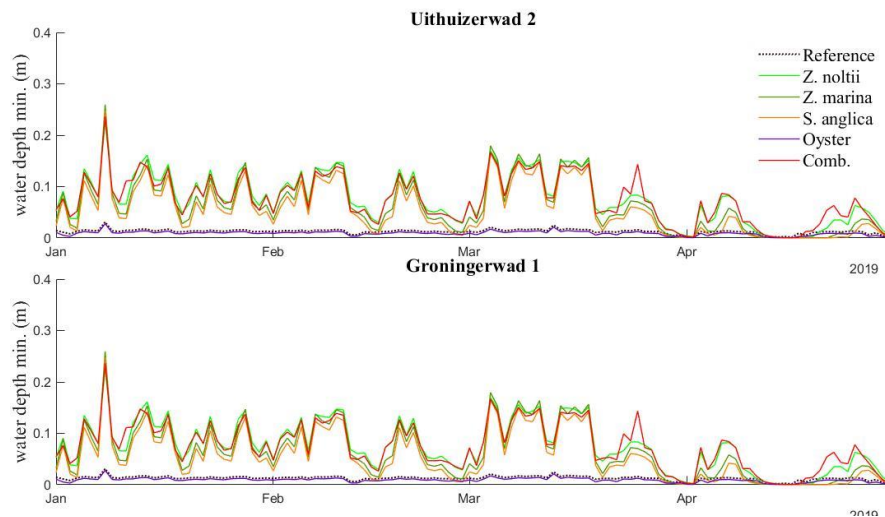
Figure 13. Daily minimum water depth (m) at the Uithuizerwad and Groningerwad coast for the different models from January till May 2019.

3.3. NbS and erosion

The bed shear stress gives an indication of the locations which are most susceptible to erosion, with higher values showing susceptibility to erosion and low values areas where sedimentation takes place. It was found that the range of bed shear stress values in the x- and y-direction at the observation points decreased when NbS were present (Figure 14). The oyster reef showed the lowest decline in the range of shear stress values compared to the reference model, while the seagrass and salt marsh species showed the highest decline in the range (Figure 14).
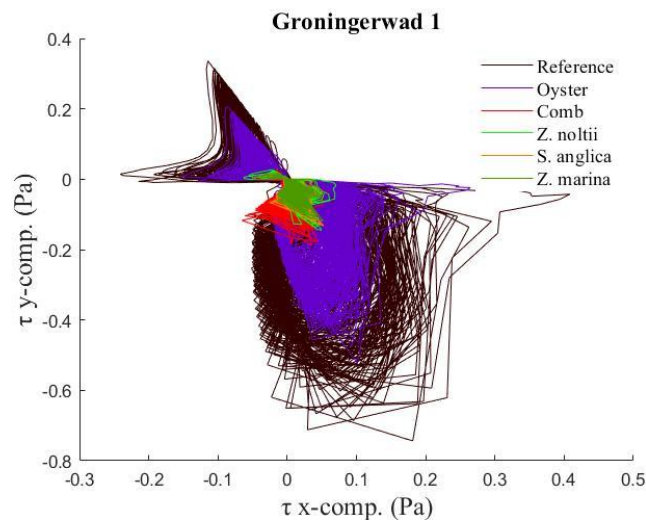
Figure 14. Bed shear stress (Pa) x- and y-component for the different NbS for the whole model period at the Groningerwad 1 coastal observation point.

23

The daily bed shear stress peak values were lower for the NbS than the reference model (Figure 15). At the observation points in the Uithuizerwad area lower maximum peak shear stress values were reached than in the Groningerwad (Figure 15). The reference model had an average peak value of 0.09 Pa (SD: 0.04) in the x-direction for the Uithuizerwad observation points, while the Groningerwad 0.38 Pa (SD: 0.19; Table B 6). In the y-direction this was 0.13 and 0.18 Pa respectively (Table B 7). The oyster reef had the highest daily mean peak values from the NbS over the study period (Table B 6).
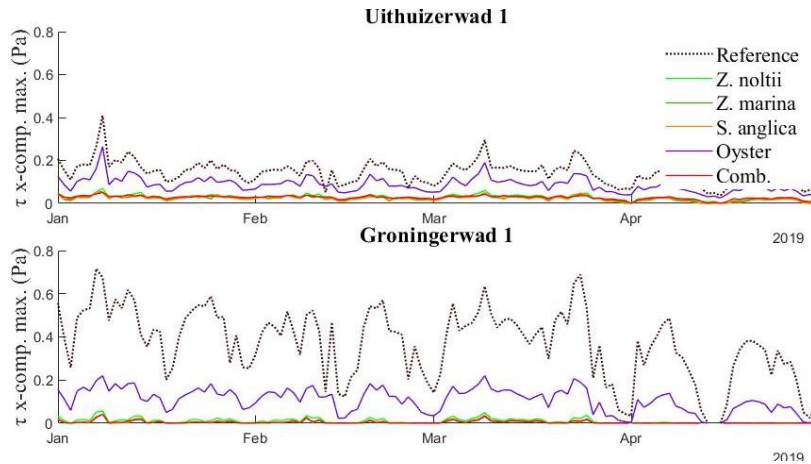
Figure 15. Daily peak bed shear stress (Pa) values of the x-component at the coastal observation points for the different NbS. The y-component peak values are shown in Figure A 3.

Spatially the bed shear stress showed higher magnitudes in areas with a high water depth (Figure 16). Therefore, the highest bed shear stress values were reached in the deep channel at the eastern side of the study area.
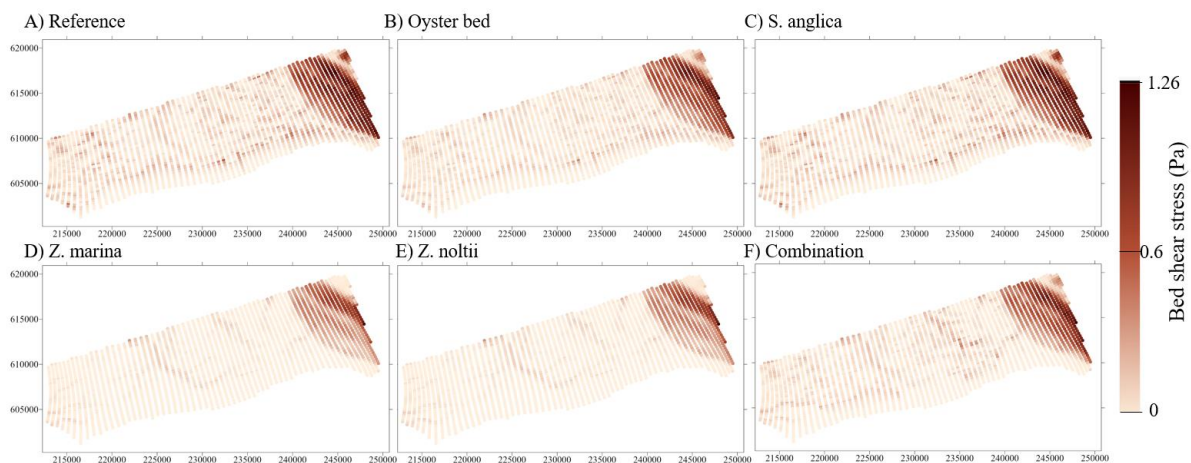
Figure 16. Bed shear stress magnitude (Pa) on the 30th of April 2019 in the study area for the different NbS. Darker values indicate areas with higher bed shear stress values and therefor higher susceptibility to erosion.

3.4.   Scenario analysis

When looking at the daily trend of the flow velocity (Figure A 4), an increase in the peak velocity was found for the SLR scenarios, with the RCP8.5 scenario showing the highest increase. When a combination of NbS was present in the study area the peak velocity decreased (Figure 17). Between the scenarios with and without a combination of NbS present, a difference in the mean peak velocity of 0.15 m s^{-1} at the coast and 0.03 m s^{-1} in the Wadden Sea was found (Table B 8). Therefore, the effect of NbS on the flow velocity was larger at the coast than at locations further away from the coast (Figure 17).
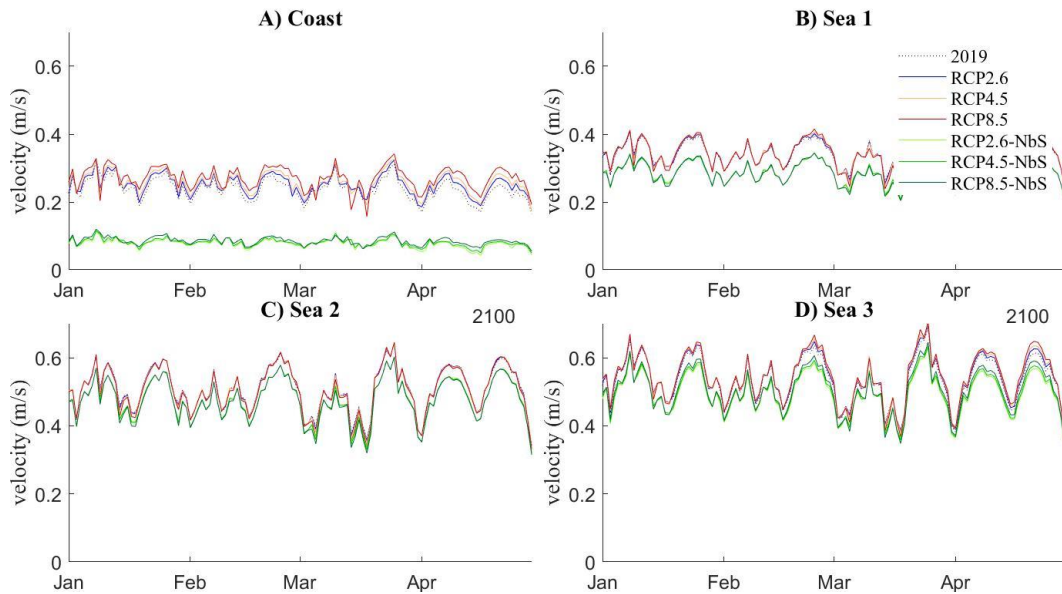
Figure 17. Daily peak velocity (m s⁻¹) for the different scenarios with and without NbS at the cross sections from January to May 2100.

The increased SLR resulted in an increase in the peak water depths at the coast, with the highest water depths for the RCP8.5 scenario (Figure A 5). The presence of NbS resulted in lower peak water depth values at the Groningerwad coast (Figure 18; Table B 9). The NbS decreased the peak water depth with 12% for the RCP2.6 scenario, while only with 3% for the RCP8.5 scenario. For the Uithuizerwad, a slight to no difference was found in the peak water depth values when NbS were present, but a decrease in the length of time that the peak values were reached was observed (Figure 18). Additionally, the NbS resulted in higher minimum water depths (Figure 19). For the scenarios with no NbS present dry periods were present at the coastal points. However, when NbS were added, the coastal zone stayed inundated during the whole study period.
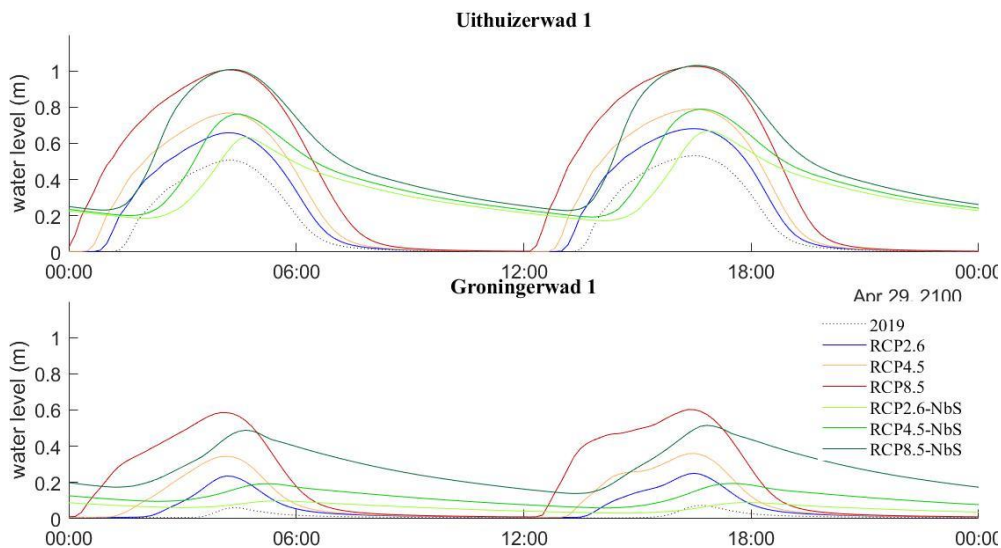
Figure 18. Water depth (m) for the SLR scenarios with and without NbS at the Uithuizerwad and Groningerwad coast on the 29ᵗʰ of April 2100.
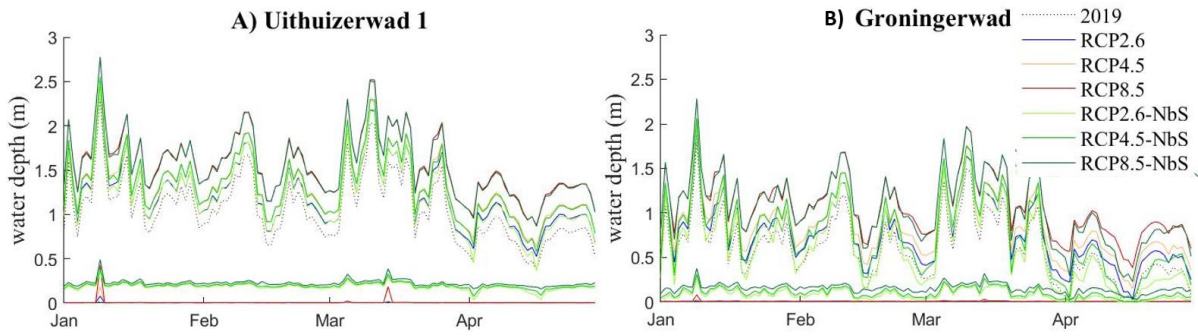
Figure 19. Maximum and minimum daily water depth for the SLR scenarios with and without NbS at the Uithuizerwad and Groningerwad coast from January till May 2100.

The bed shear stress peak values increased for the SLR scenarios (Figure 20), indicating that higher levels of erosion took place at the coast with increased water levels. However, the presence of NbS decreased the bed shear stress peak values, from a range of 0.8-0.1 Pa when no NbS were present to 0.01 Pa when NbS were present in the study area (Figure 20).
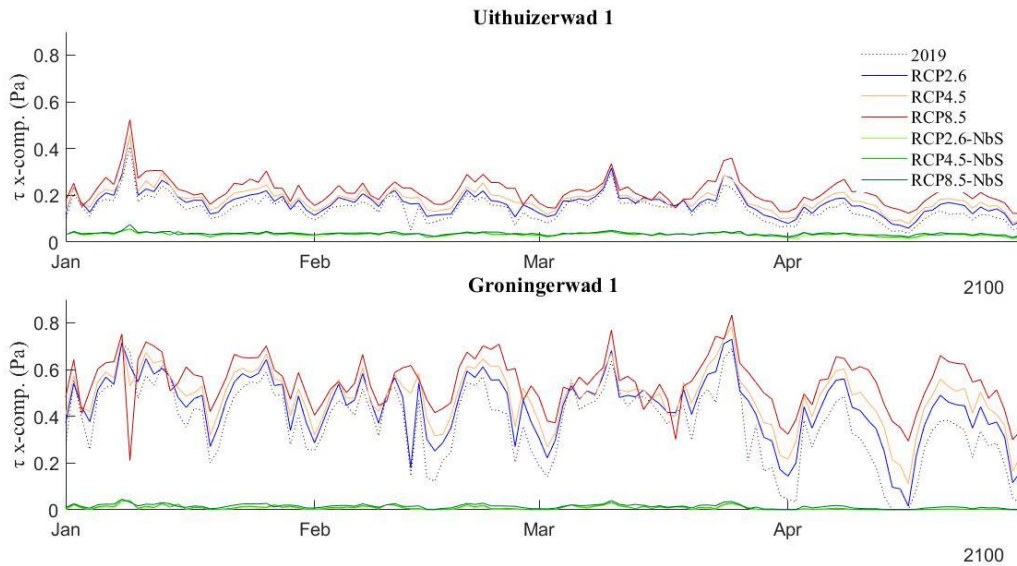
Figure 20. The maximum daily bed shear stress (Pa) x-component for the different scenarios at the different coastal observation points from January till May 2100.

3.5. Sensitivity analysis

Peak flow velocities decreased with increased heights (h_v), densities (n) and drag coefficients (C_d) of the NbS (Figure 21). When no NbS were present the flow velocity had an average peak velocity of 0.27 m s^{-1} (SD: 0.03). H_v resulted in the largest decrease in the peak velocities (0.03 m s^{-1}, SD: 0.02; Table B 10). With very high densities (n=1000) the peak velocity averaged at 0.04 m s^{-1} (SD=0.02; Table B 11), while for large drag coefficients (C_d=2) they averaged at 0.06 m s^{-1} (SD: 0.02; Table B 12). The different C_b values did not decrease the peak velocity of the model, only an unrealistically low C_b value (C_b=1) had an impact on the peak velocities (Table B 13). Therefore, the peak flow velocity was found to be most sensitive to the height of the NbS and least to the background roughness parameter.
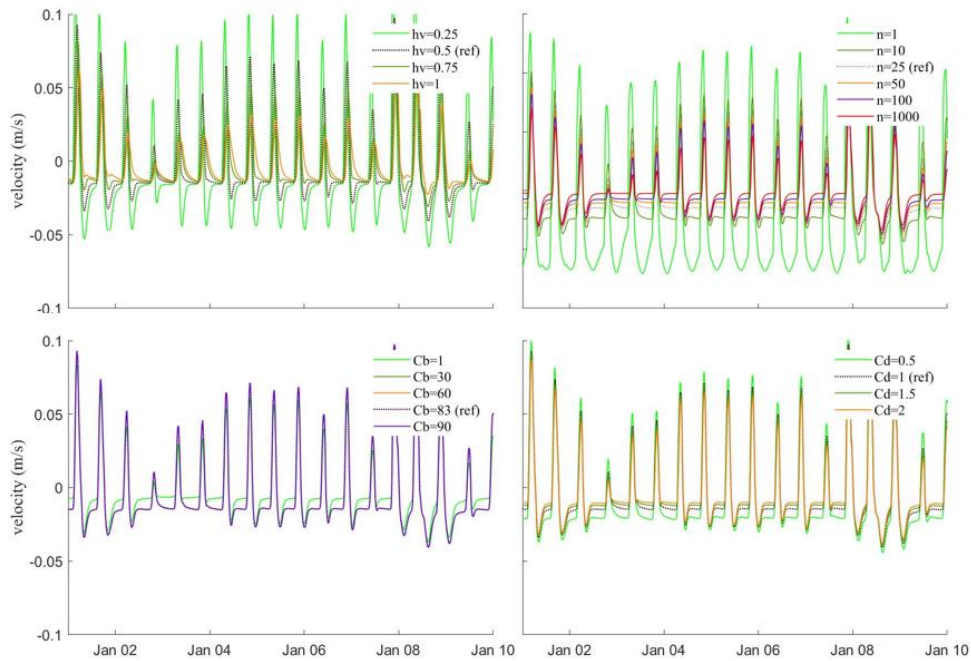
Figure 21. Flow velocity (m s⁻¹) for different height (hᵥ), density (n), background roughness (Cᵦ) and drag coefficient (Cₐ) parameter values to represent NbS in the model, from 1-10 January 2019 at the coast of the study area.

The peak water depth also decreased with increased h_v, n and C_d values (Figure 22).When no NbS were present in the study area, water depths peaked at an average of 0.93 m (SD: 0.27) from the first till the 10th of January. When NbS of one metre were present the peak water depths only reached 0.43 m (SD: 0.03; Table B 10). With high Cd values peak water depths of 0.66 m were reached (SD: 0.06; Table B 12). With an extreme density (n=1000) peak water depths increased compared to lower densities (n=25-100), from 0.66 m (SD: 0.02) to 0.71 m (SD: 0.02; Table B 11). The C_b only influenced the peak water depth values when very low values were present (C_b=1; Table B 13). Furthermore, the very low C_b increased the water depth when no peaks were present (Table B 13). Consequently, peak water depths were most sensitive to the height of the NbS and drag coefficient, while they were less sensitive to the density and background roughness parameters.
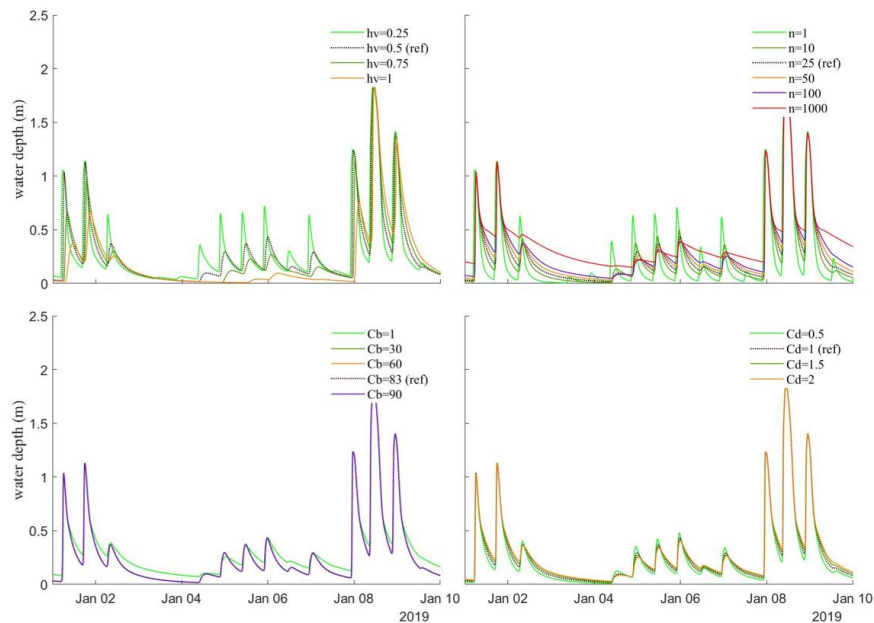
Figure 22. Water depth (m) for different heights of NbS (hᵥ), densities (n), background roughness (Cᵦ) and drag coefficients (Cₐ) values from 1-10 January 2019 at the Uithuizerwad 2 observation point.

27

4. Discussion

This thesis aimed to identify whether the implementation of coastal NbS can increase the coastal protection of intertidal zones. For this the interaction of seagrass meadows (*Z. noltii* and *Z. marina*), salt marshes (*S. Anglica*) and oyster beds (*O. edulis*) with the hydrodynamics were schematised in the Delft3D-FM Flow model in the Ems-Dollard estuary. The results indicate that, through increasing the bed roughness, the presence of NbS in the Groningerwad and Uithuizerwad area decrease the peak flow velocity and water levels that reach the coastline. Furthermore, the study demonstrates that salt marsh and seagrass species decrease the daily peak flow and water levels more than oyster beds do. The bed shear stress peak values also decrease with the presence of NbS, indicating that the period with elevated levels of erosion decreases. These results confirm the hypotheses that NbS decrease the flow velocity, water depth and level of erosion. With future SLR, the flow velocities and water levels increase at the coast, enhancing the need for a reduction in the peak levels by NbS. The NbS were found to decrease the increased peak values with SLR, but the question remains whether this will be sufficient to protect the coast from flooding with future climate change.

4.1. Coastal protection potential of NbS

When NbS are present, the peak flow velocity was found to decline by 70% at the coast when salt marsh and seagrass meadows are present, while only by 12% when oyster beds are present. Other studies also found a reduction in the flow velocity when NbS are present. Van Veelen et al. (2010) found a reduction in the depth-averaged flow velocity when salt marshes were present in an estuary modelled by Delft3D-FM (van Veelen et al., 2019). From measurements in salt marsh vegetation, flow velocities were found to be a magnitude lower than those in surrounding mudflats in the Western Scheldt estuary (Bouma et al., 2005). For the *Spartina alterniflora* salt marsh species, a 50% reduction of flow velocity was found in the canopy (Leonard & Croft, 2006). For the *Z. marina* seagrass, a 70-90% reduction in the near-bottom flow velocity was measured in a coastal bay in Virginia (Hansen & Reidenbach, 2012). For oyster reefs only a small reduction in the peak flow velocity was found in this study, however, others found a reduction of up to 40% in the mean horizontal flow profile of healthy oyster reefs (Kitsikoudis et al., 2020). Furthermore, when NbS are present, the vertical component of the flow was found to be attenuated more strongly than the horizontal component (Leonard & Croft, 2006). However, the vertical component of the flow is not considered in the depth-averaged model used for this research as the Boussinesq assumption is made. By using a depth-averaged model, there is also an underestimation present in the effect of NbS on the near-bed currents (Keyzer et al., 2020), while these were found to be attenuated most when NbS are present (Hansen & Reidenbach, 2012).

The NbS were found to decrease the peak water depth at the coast. The salt marsh and seagrass species resulted in a decrease of 6-34% (depending on the location), while the oyster reef resulted in a 5-8% decrease in the peak water depth at the coast compared to when no NbS were present in the Groningerwad and Uithuizerwad area. This indicates that the tidal amplitude is decreased at the coast by the presence of NbS. Best et al. (2018) also found that when salt marsh vegetation is present in an area the tidal amplitude decreases (Best et al., 2018). By decreasing the peak velocity and water depth, NbS reduce the water force that reaches the coast. Consequently, the dikes that are present in the Groningerwad and Uithuizerwad are exposed to less hydrodynamic forces. This indicates that the need for maintenance of the dikes can be reduced by the presence of NbS in the foreshore.

An unexpected result for the water depth with the presence of salt marsh and seagrass meadows was that the intertidal zone stayed inundated for a longer period of time. Although water depths did reach low levels of about 10 cm during low tide, the coastal zone stayed flooded. Temmerman et al. (2005) also observed that when water levels were low, vegetated areas flooded more than unvegetated areas (Temmerman et al., 2005). More specifically, they observed that when the water level was below the top of the vegetation, flow routing took place from unvegetated to vegetated tidal marsh areas

(Temmerman et al., 2005). As water depths observed here during low tides were lower than the height of the NbS, flow routing could have been the explaining factor. With an increase in the length that the area stays flooded, inundation stresses on the NbS increase. Consequently, this could lead to a decrease in the quality of the Uithuizerwad and Groningerwad area as a habitat for the salt marsh and seagrass species, decreasing the coastal protection potential of these NbS. However, this is without taking into consideration the effect of NbS on the amount of sedimentation.

The salt marsh and seagrass species resulted in a reduction in the bed shear stress peak values at the coast of 80-95%, while the oyster reef 40-60%. This reduction indicates that the system may have shifted from an erosional environment to one that promotes the deposition of suspended sediments. As the amount of suspended sediment decreases, more light is able to reach the vegetation and promote growth (Paul, 2018), which could lead to a positive feedback loop for the growth of NbS. Other studies also found that seagrass species reduce the bed shear stress and thereby stabilise sediments (Christianen et al., 2013; Hansen & Reidenbach, 2012; Paul, 2018; Widdows et al., 2008). Furthermore, the bed shear stress was found to decrease below the critical shear stress when NbS are present (Hansen & Reidenbach, 2012; Widdows et al., 2008). The critical shear stress is the bed shear stress value above which sediments are mobilised and below which they are stabilised. For the *Z. marina* species an 80% reduction was found in the bed shear stress compared to an unvegetated area (Hansen & Reidenbach, 2012). The critical shear stress (0.4 Pa) was not exceeded for 80% of the time in the eelgrass meadow (Hansen & Reidenbach, 2012). If this critical shear stress is used for the results of this study, the shear stress for *Z. marina* stays below the critical shear stress value during the entire studied period. For a *Z. noltii* meadow in Sylt, Germany, the bed shear stress was also found to stay below the critical shear stress (0.1-1 Pa) and increased with higher shoot densities (Widdows et al., 2008). When using the lowest critical shear stress found in this study (0.1 Pa; Widdows et al., 2008), the critical shear stress was not exceeded by the shear stress values observed for *Z. noltii* in this study either. Furthermore, the depth averaged model used in this study was found to slightly overestimate the bed shear stress, as it does not resolve the enhanced reduction of velocity by the vegetation that is observed near the bed (Horstman et al., 2015).

The combination of NbS did not increase the coastal protection more than when one NbS was present in the study area. This was due to the spatial separation of the NbS and not considering interactions between the NbS. For example, the same density was assumed for the NbS as when they were separately present, however synergies between the NbS could lead to an increase in their density. For example, the habitable range of oysters was found to increase by the presence of salt marshes in the Western and Eastern Scheldt estuary (Fivash et al., 2021). Furthermore, oyster reefs were found to reduce the erosion of salt marshes and increase the growth of the vegetation (Paul, 2018; Ysebaert et al., 2018). Seagrasses were found to increase the water quality, thereby increasing the habitat quality of oysters (Kobayashi et al., 2021). This indicates that a combination of NbS can increase their extent and quality, and thereby their coastal protection potential. For example, Keyzer et al. (2020) indicate that the interdependence between NbS is a key factor in the resilience of the system to SLR. However, more research is needed to determine the extent to which a combination of NbS can increase their coastal protection potential by taking the synergies between NbS into account.

By implementing the NbS in the Delft-3D-FM Flow model through the trachytope functionality, the roughness in the study area was increased. This was consequently found to decrease the flow velocity and the water depth peak values. By partly implementing drag by NbS in the momentum balance, the trachytope functionality decreased the bed shear stress, indicating a decrease in the rate of erosion in the area. Although the model is a limited representation of the real-life situation, measurements at seagrass, salt marsh and oyster beds found the here simulated coastal protection effects by NbS to be present as well (e.g., Bouma et al., 2005; Hansen & Reidenbach, 2012; Ysebaert et al., 2018).

4.2. SLR scenarios and NbS

The SLR scenarios increased the peak flow velocity and water depth, which were subsequently reduced by the presence of NbS. Nevertheless, the question remains whether this decrease is sufficient to protect the coast from flooding. With the highest SLR scenario (RCP 8.5) the peak velocity decreased from 0.27 to 0.09 m s^{-1}, which is lower than the modelled value without NbS in 2019. However, the peak water depth only decreased with 2-12% at the coast when NbS were present in the future SLR scenarios. Thus, the RCP8.5 scenario for 2100 still reached 50 cm higher peak values at the coast than the model for 2019. This indicates that if high levels of climate change will be reached by 2100, NbS can help with coastal protection, but additional measures will need to be taken to ensure the safety of the coastline.

A key effect of the NbS is the increase in the bed level they result in, as this determines whether NbS can keep up with future SLR. However, in the model used for this study the changes in geomorphological processes were not taken into account. Best et al. (2018) did take geomorphological processes into account in a Delft3D-FM model for salt marshes (Best et al., 2018). They found that the rate at which the bed level increases is insufficient to keep up with the SLR predicted with the RCP8.5 scenario by 2100 (Best et al., 2018). However, as the increase in bed level is dependent on the sediment supply, it could be increased by adding external sediments to the system (Best et al., 2018; Wang et al., 2018). For example, artificial sand nourishment can increase the capacity of the system to keep up with the rising sea levels (Stronkhorst et al., 2018).

With the presence of NbS in SLR scenarios, permanent coverage of water was found at the coastline. This indicates that the area has shifted from an intertidal to a subtidal system. Other studies have also observed this transition in the Wadden Sea system with future SLR (Becherer et al., 2018; Dissanayake et al., 2012; Wang et al., 2018). With the RCP2.6 scenario a 3.5% loss, while with the RCP8.5 a 38% loss was found of tidal flats in the Wadden Sea (Wang et al., 2018). This will potentially have dramatic consequences on the ecosystem present in the Wadden Sea (Wang et al., 2018), and could decrease the effectiveness of the proposed NbS. For example, the zonal sequence of salt marshes is dependent on the duration and frequency of inundations, and have been found to shift landwards where SLR takes place (Metzing, 2010; Willemsen et al., 2022). However, this landward retreat of NbS is limited in the Wadden Sea by the presence of dikes. Furthermore, with rising temperatures caused by climate change, a shift in species coastwards and northwards is predicted in the Wadden Sea, which will change the species composition and biotic interactions in the ecosystems (Metzing, 2010). It is therefore important for future research that study the effectiveness of NbS for coastal protection with SLR, to also consider the effect of the higher sea levels on the NbS and the effect that an increase in the duration and frequency of inundation has on the system.

The findings of this thesis indicate that NbS can help with coastal protection, by reducing the water level and flow velocity reaching the coast in the Uithuizerwad and Groningerwad. However, to ensure the highest flood safety, a hybrid coastal protection approach is suggested. A hybrid approach means that NbS are combined with civil-engineered structures (van der Nat et al., 2016). For example, in the Uithuizerwad and Groningerwad area, salt marsh, seagrass and oyster reefs can be used as a foreshore coastal protection option. The NbS thereby function as a buffer to the incoming hydrodynamic forces and reduce the forces that reach the coastline. But next to these NbS, dikes are still needed to ensure maximal safety from flooding. By taking a hybrid approach, the resilience of the coastal system to SLR is also increased.

Therefore, the cooperation of multiple disciplines and actors is needed for coastal protection. For example, there is a need for both ecological and engineering knowledge in the design of coastal protection measures. Ecologists can help with the design of the NbS, to ensure their ecological quality and thereby coastal protection potential, while hydraulic engineers can help with the design of the civil-engineered structures. Furthermore, a broader range of stakeholders need to be involved within the design process, to ensure that societal values are considered in the coastal protection measure.

4.3. Sensitivity analysis

The results of the sensitivity analysis revealed that the flow velocity and water depth were most sensitive to the height of the NbS, from the parameters used for the NbS in the model. The density of the NbS and the drag coefficient also influenced coastal protection, but to a lesser degree. The background roughness had no to a very little effect. As the oyster reefs were parameterised to have the smallest height, this could explain why they were found to have lower coastal protection effects than the salt marsh and seagrass vegetation. Temmerman et al. (2005) also found that vegetation height is the controlling factor for the water depth over salt marshes (Temmerman et al., 2005). Furthermore, the effect of vegetation density was found to be more clearly visible at low density ranges (0-10% coverage) than high densities (Temmerman et al., 2005). Bouma et al. (2010) also found that the drag force exerted by the vegetation on the flow, is independent of the vegetation density and relatively constant in space, but is a species-specific characteristic (Bouma et al., 2010). However, Karamouz et al. (2022) found that the drag coefficient is the determining factor for the drag force of mangrove and kelp vegetation in the Delft3D model. Therefore, when parameterising NbS in hydrodynamic models, special attention must be paid to determining the height of the NbS.

4.4. Other uncertainties and limitations

The main assumption that was made for this study is that the whole Uithuizerwad and Groningerwad area are covered by NbS. In reality, the NbS need specific conditions to colonise an area and form healthy systems. For example, oyster reefs need hard substrates to settle on (e.g. shells or artificial structures), sufficient water quality, and shallow water conditions (Fivash et al., 2021; Smaal et al., 2015). Furthermore, *O. edulis* has a very rare occurrence in the Wadden Sea (Smaal et al., 2015), due to which significant restoration efforts need to be taken. The density that is reached with restoration projects of NbS is often very low. For example, for *O. edulis* only 0.6-6.8 oysters per m² were present in the North sea (Christianen et al., 2018). For the *Z. marina* species a maximum density of 1.8 plants per m² was achieved by a restoration project in the Uithuizerwad area (Govers et al., 2018), which is significantly lower than the density used for this study (1451.37 shoots per m²). More established NbS were also found to have a lower density than the density used for this study. For example, the shoot density of a *Z. marina* meadow in the Ems Estuary was found to peak at 7.8 flowering shoots per m² (Erftemeijer et al., 2008). Therefore, it is more realistic to assume that lower ranges and densities will be reached by NbS in the Uithuizerwad and Groningerwad area by future restoration projects.

Another assumption which was made is that the NbS do not change over time. Although the trachytope functionality in the Delft3D-FM model does allow for spatial heterogeneity in the vegetation, it is not possible to make the NbS temporally variable. Due to this, the effect that the hydrodynamic conditions have on the NbS were not considered. To do so, a Dynamic Vegetation Model could be coupled to the model. Such a model is currently under development for the Delft3D-FM model (Dijkstra, 2022). By coupling the hydrodynamic model with a Dynamic Vegetation Model, the parameters of the vegetation can be calculated based on changing environmental conditions. For example, the observed elevated water depths could be coupled with a decrease in light availability and thereby mortality of the NbS.

By making the NbS temporally variable and dependent on the hydrodynamic conditions, their coastal protection potential will also change over time. This is important, because the effectiveness of the coastal protection of seagrasses and salt marshes has been found to change over time (Koch et al., 2009; Ondiviela et al., 2014). For example, the density, aboveground biomass and height of seagrasses has been found to be low during winter, decreasing their coastal protection potential (Koch et al., 2009; Paul & Amos, 2011). However, during winter the most extreme hydrodynamic conditions are present in the Wadden Sea, with coastal protection therefore being the most important during this time. Even though the winter period was simulated in this study, a healthy ecosystem was assumed to be present, thus leading to an overestimation in the coastal protection potential of seagrasses and salt marshes. For future research on NbS it would therefore be an important aspect to consider the temporal variability of NbS by, for example, coupling a hydrodynamic model with a Dynamic Vegetation Models.

Another aspect which was assumed to be constant over time, is the drag coefficient of NbS. This is an oversimplification as it neglects the stem behaviour of salt marshes and seagrasses under different hydrodynamic conditions (Familkhalili & Tahvildari, 2022). For example, the drag coefficient was found to increase with water depths and decrease with the steepness in wave conditions (He et al., 2018). The flow velocity also impacts the drag coefficient, by causing a sway in the vegetation (Paul & Amos, 2011; Zeller et al., 2014). By the sway in vegetation the frontal area, height of the vegetation, and thereby the drag exerted on the flow decreases. The Baptist et al. (2007) method in the Delft3D-FM model assumes rigid vegetation and thereby does not consider the flexibility of the vegetation. Furthermore, a linear relation between the drag force and the square of velocity is assumed, while for flexible plants a linear increase between the drag force and flow velocity is observed (Armanini et al., 2005). Several studies have shown that by the coupling of a Dynamic Vegetation Model (Familkhalili & Tahvildari, 2022; Karamouz et al., 2020) or making the drag coefficient value dependent on wave conditions (Christie et al., 2018; Losada et al., 2016), a more realistic drag on the flow by flexible vegetation can be simulated. Therefore, for future research the incorporation of the stem flexibility by a variable drag coefficient is important for modelling the effect of salt marsh and seagrasses on the hydrodynamics.

Another suggestion for further research is to determine the properties of the NbS and hydrodynamics in the Uithuizerwad and Groningerwad area through a field study. For this thesis, assumptions were made in the parameterisation of the NbS by not taking measurements at location. Parameters that were determined in other studies were used. However, the specific conditions present at the Uithuizerwad and Groningerwad could result in different heights, densities and drag coefficients of the NbS. For some of the parameters, values from different species had to be used, because of a limitation in data availability for the studied species. By performing measurement on location, the spatial heterogeneity of the NbS could be taken into account in the model environment. This way the assumption of uniform height, density and drag coefficient which was made in this study would not have to be made. Measurements would also allow the NbS within the model to be calibrated and validated against local data. Additionally, the critical bed shear stress could be measured with field observations.

Another uncertainty lies within the parameters that were used for the scenarios by 2100. For the RCP8.5 scenario the SLR projections have a 5-95% uncertainty of 0.36 m, which indicates that SLR could increase to 1.12 m instead of the here applied 0.76 m (Vermeersen et al., 2018). Uncertainties in the SLR scenarios lie within uncertainties in the internal climate variability (e.g., ENSO), emission pathways, climate models and potential ice-mass loss from Antarctica and Greenland (Haasnoot et al., 2020; Vermeersen et al., 2018). For the sedimentation rate an extrapolation was made from the 1926-2015 average, however, this is highly dependent on the sediment availability and transport rate within the area and is spatially variable. The subsidence rate projections also had a 50% uncertainty and are highly dependent on uncertain human induced processes in the area (e.g., gas extraction). Furthermore, other effects of climate change which could affect the hydrodynamic conditions (e.g., storm surges, river discharge, precipitation) were not considered in this study.

Another important factor of NbS which was not considered in this research, is the ecosystem services they provide in addition to coastal protection. For example, all the NbS studied here have been found to increase the carbon storage of an area (Duarte et al., 2013; Thomas et al., 2022). By storing carbon, the NbS help with climate change mitigation in addition to adaptation. Globally, salt marshes and seagrasses were estimated to bury between 50 to 200 Tg carbon yr^{-1} (Duarte et al., 2013). Furthermore, other ecosystem services that the studied NbS can provide are: water purification, nitrogen cycling, food provision and recreation (Kobayashi et al., 2021; Moraes et al., 2022; Rozema et al., 2002).

5. Conclusion and Recommendations

This research found that salt marshes (*S. Anglica*), seagrasses (*Z. marina* and *Z. noltii*) and oyster reefs (*O.* edulis) can decrease the peak flow and water level that reaches the coast. By increasing the bed roughness through the Delft3D-FM Flow model trachytope functionality in the Uithuizerwad and Groningerwad area (Dutch Wadden Sea), drag force on the flow increased, decreasing the peak velocity and water that reached the coast. Furthermore, the peak levels of the bed shear stress, which is a proxy for the amount of erosion, also decreased. However, the intertidal zone was found to stay inundated for a longer period of time when NbS were present, which could decrease the habitat suitability of the area for the NbS. Salt marsh and seagrass species were found to have comparable coastal protection potentials, while oyster beds had a lower potential. The parameter that mostly defines the coastal protection potential is the height of the NbS, with the density and drag force having a lower influence. With increasing sea level rise scenarios, NbS also decreased the peak flow velocity, water depth and rate of erosion. However, the decrease by NbS in the water level is insufficient to protect the coast from inundation with SLR by 2100. Therefore, with high levels of climate change, the NbS analysed here can help with coastal protection, but additional measures need to be taken to ensure the safety of the coastline. A hybrid approach to coastal protection is suggested, by combining the positive effects of NbS with conventional coastal engineering solutions. Furthermore, sand nourishment can be applied to the here introduced NbS, to ensure that the bed level increases at a rate that is able to keep up with future sea level rise. To conclude, this thesis found that NbS can help with coastal protection, but the amount is dependent on the type of NbS and the hydrodynamic conditions present.

Recommendations for further research are to:

- Make the representation of NbS in models temporally and spatially variable and dependent on environmental conditions (e.g., coupling of hydrodynamic models with Dynamic Vegetation Model).
- Investigate what the effect of rising sea levels and temperatures are on NbS.
- Use field data to determine the properties of the NbS for the specific location that is modelled.
- Determine and model the interdependencies that are present between NbS, and how this influences their coastal protection potential.
- Consider the effect of a higher sea level on the NbS in addition to the effect of NbS on the water level.
- Use a 3D model to also consider the effect of NbS on the vertical component of the flow and prevent the underestimation of the reduction in the near-bed flow velocity.
- Consider the limits of implementing NbS in coastal areas.
- Look whether with an artificial supply of sediment, NbS can keep up with high amounts of sea level rise.
- Determine the combined coastal protection potential of NbS and coastal engineering solutions.
- Consider and quantify the additional ecosystem services that NbS provide on top of coastal protection.

6. Bibliography

Adam, P. (1990). *Saltmarsh Ecology*. Cambridge University Press.

Agardy, T., Lead, J. A., Dayton, P., Curran, S., Kitchingman, A., Wilson, M., Catenazzi, A., Restrepo, J., Birkeland, C., Blaber, S., Saifullah, S., Branch, G., Boersma, D., Nixon, S., Dugan, P., Davidson, N., & Vörösmarty, C. (2005). Coastal Systems. In J. Baker, P. Moreno Casasola, A. Lugo, A. Suárez Rodríguez, L. Dan, & L. Tang (Eds.), *Millenium Ecosystem Assessment* (pp. 513–549). Island Press.

Anderson, M. E., & Smith, J. M. (2014). Wave attenuation by flexible, idealized salt marsh vegetation. *Coastal Engineering*, *83*, 82–92. https://doi.org/10.1016/j.coastaleng.2013.10.004

Armanini, A., Righetti, M., & Grisenti, P. (2005). Direct measurement of vegetation resistance in prototype scale. *Journal of Hydraulic Research*, *43*(5), 481–487. https://doi.org/10.1080/00221680509500146

Baptist, M. J. (2005). Modelling floodplain biogeomorphology. In *Doctoral Dissertation*. Delft University of Technology.

Baptist, M. J., Babovic, V., Uthurburu, J. R., Keijzer, M., Uittenbogaard, R. E., Mynett, A., & Verwey, A. (2007). On inducing equations for vegetation resistance. *Journal of Hydraulic Research*, *45*(4), 435–450. https://doi.org/10.1080/00221686.2007.9521778

Barbier, E. B., Hacker, S. D., Kennedy, C., Koch, E. W., Stier, A. C., & Silliman, B. R. (2011). The value of estuarine and coastal ecosystem services. *Ecological Monographs*, *81*(2), 169–193. https://doi.org/10.1890/10-1510.1

Barros, V. R., Field, C. B., Dokken, D. J., Mastrandrea, M. D., Mach, K. J., Bilir, T. E., Chatterjee, M., Ebi, K. L., Estrada, Y. O., Genova, R. C., Girma, B., Kissel, E. C., Levy, A. N., MacCracken, S., Mastandrea, P. R., & White, L. L. (2014). Technical Summary. In *Climate Change 2014: Impacts, Adaptation, and Vulnerability. Part A: Global and Sectoral Aspects. Contribution of Working Group II to the Fifth Assessment Report of the Intergovernmental Panel on Climate Change* (pp. 35–94). Cambridge University Press.

Barua, D. K. (2020). Seabed roughness of coastal waters. In C. W. Finkl & C. Makowski (Eds.), *Encyclopedia of Coastal Science*. Springer International Publishing. https://doi.org/10.1007/978-3-319-48657-4

Basismonitoringwadden. (2020). *Wadden viewer - Groningen-Friesland Vegetatiestructuur*. https://viewer.openearth.nl/wadden-viewer/

Becherer, J., Hofstede, J., Gräwe, U., Purkiani, K., Schulz, E., & Burchard, H. (2018). The Wadden Sea in transition - consequences of sea level rise. *Ocean Dynamics*, *68*(1), 131–151. https://doi.org/https://doi.org/10.1007/s10236-017-1117-5

Beck, M. W., Brumbaugh, R. D., Airoldi, L., Carranza, A., Coen, L. D., Crawford, C., Defeo, O., Edgar, G. J., Hancock, B., Kay, M. C., Lenihan, H. S., Luckenbach, M. W., Toropova, C. L., Zhang, G., & Guo, X. (2011). Oyster Reefs at Risk and Recommendations for Conservation, Restoration, and Management. *BioScience*, *61*(2), 107–116. https://doi.org/10.1525/bio.2011.61.2.5

Best, U. S. N. (2017). *Process-based modelling of the impact of sea level rise on salt marsh & mangrove fringe-mudflat morphodynamics [An assessment of the decadal triggers for morphological evolution and restoration methods]* [Delt: UNESCO-IHE Institute for Water Education]. https://doi.org/10.25831/rght-5D21

Best, U. S. N., Van der Wegen, M., Dijkstra, J., Willemsen, P. W. J. M., Borsje, B. W., & Roelvink, D. J. A. (2018). Do salt marshes survive sea level rise? Modelling wave action, morphodynamics and vegetation dynamics. *Environmental Modelling & Software*, *109*, 152–166. https://doi.org/10.1016/j.ensoft.2018.08.004

Borum, J., Duarte, C. M., Krause-Jensen, D., & Greve, T. M. (2004). *European seagrasses: an introduction to monitoring and management*. EU project Monitoring and Managing of European Seagrasses.

Bos, A. R., Bouma, T. J., de Kort, G. L. J., & Van Katwijk, M. M. (2007). Ecosystem engineering by annual intertidal seagrass beds: Sediment accretion and modification. *Estuarine, Coastal and Schelf Science*, *74*, 344–348. https://doi.org/10.1016/j.ecss.2007.04.006

Bostrom, C., & Bonsdorff, E. (2000). Zoobenthic community establishment and habitat complexity - the importance of seagrass shoot-density, morphology and physical disturbance for faunal recruitment. *Marine Ecology Progress Series*, *205*, 123–138. https://doi.org/10.3354/meps205123

Bouma, T. J., de Vries, M. B., & Herman, P. M. J. (2010). Comparing ecosystem engineering efficiency of two plant species with contrasting growth strategies. *Ecology*, *91*(9), 2696–2704. https://doi.org/10.1890/09-0690.1

Bouma, T. J., de Vries, M. B., Low, E., Kusters, L., Herman, P. M. J., Tánczos, I. C., Temmerman, S., Hesselink, A., Meire, P., & Van Regenmortel, S. (2005). Flow hydrodynamics on a mudflat and in salt marsh vegetation: Identifying general relationships for habitat characterisations. *Hydrobiologia*, *540*(1–3), 259–274. https://doi.org/10.1007/S10750-004-7149-0

Brière, C., Janssen, S. K. H., Oost, A. P., Taal, M., & Tonnon, P. K. (2017). Usability of the climate-resilient nature-based sand motor pilot, The Netherlands. *Journal of Coastal Conservation*, *22*, 491–502. https://doi.org/10.1007/s11852-017-0527-3

Cannaby, H., Palmer, M. D., Howard, T., Bricheno, L., Calvert, D., Krijnen, J., Wood, R., Tinker, J., Bunney, C., Harle, J., Saulter, A., O'Neill, C., Bellingham, C., & Lowe, J. (2016). Projected sea level rise and changes in extreme storm surge and wave events during the 21st century in the region of Singapore. *Ocean Science*, *12*(3), 613–632. https://doi.org/10.5194/os-12-613-2016

Cheong, S. M., Silliman, B., Wong, P. P., Van Wesenbeeck, B., Kim, C. K., & Guannel, G. (2013). Coastal adaptation with ecological engineering. *Nature Climate Change*, *3*(9), 787–791. https://doi.org/10.1038/nclimate1854

Chiu, Y.-Y., Raina, N., & Chen, H.-E. (2021). Evolution of Flood Defense Strategies: Toward Nature-Based Solutions. *Environments*, *9*(1). https://doi.org/10.3390/environments9010002

Christianen, M. J. A., Lengkeek, W., Bergsma, J. H., Coolen, J. W. P., Didderen, K., Dorenbosch, M., Driessen, F. M. F., Kamermans, P., Reuchlin-Hugenholtz, E., Sas, H., Smaal, A., van den Wijngaard, K. A., & van der Have, T. M. (2018). Return of the native facilitated by the invasive? Population composition, substrate preferences and epibenthic species richness of a recently discovered shellfish reef with native European flat oysters (Ostrea edulis) in the North Sea. *Marine Biology Research*, *14*(6), 590–597. https://doi.org/10.1080/17451000.2018.1498520

Christianen, M. J. A., van Belzen, J., Herman, P. M. J., van Katwijk, M. M., Lamers, L. P. M., van Leent, P. J. M., & Bouma, T. J. (2013). Low-Canopy Seagrass Beds Still Provide Important Coastal Protection Services. *PLoS ONE*, *8*(5). https://doi.org/10.1371/journal.pone.0062413

Christie, E. K., Möller, I., Spencer, T., & Yates, M. (2018). Modelling Wave Attenuation due to Saltmarsh Vegetation Using a Modified SWAN model. *Coastal Engineering Proceedings*, *1*(36). https://doi.org/10.9753/icce.v36.papers.73

Church, J. A., Clark, P. U., Cazenave, A., Gregory, J. M., Jevrejeva, S., Levermann, A., Merrifield, M. A., Milne, G. A., Nerem, R. S., Nunn, P. D., Payne, A. J., Pfeffer, W. T., Stammer, D., & Unnikrishnan, A. S. (2013). Sea level change. In T. F. . Stocker, D. . Qin, G.-K. . Plattner, & et al. (Eds.), *Climate change 2013: The physical science basis. Contribution of Working Group I to the Fifth Assessment Report of the Intergovernmental Panel on Climate Change* (pp. 1137–1216). Cambridge University Press.

Cobacho, S. P., Wanke, S., Konstantinou, Z., & El Serafy, G. (2020). Impacts of shellfish reef management on the provision of ecosystem services resulting from climate change in the Dutch Wadden Sea. *Marine Policy*, *119*. https://doi.org/10.1016/j.marpol.2020.104058

de Jong, D. J., Van Katwijk, M. M., & Brinkman, A. G. (2005). *Kansenkaart Zeegras Waddenzee - Potentiële groeimogelijkheden voor zeegras in de Waddenzee*. https://edepot.wur.nl/174533

de Jonge, V. J., de Jong, D. J., & van Katwijk, M. M. (2000). Policy plans and management measures to restore eelgrass (Zostera marina L.) in the Dutch Wadden Sea. *Helgoland Marine Research*, *54*(2), 151–158. https://doi.org/10.1007/s101520050013

de Vriend, H. J., van Koningsveld, M., & Aarninkhof, S. (2014). "Building with nature": The new Dutch approach to coastal and river works. *Civil Engineering*, *167*(1), 18–24. https://doi.org/10.1680/cien.13.00003

Deltares. (2022). *D-Flow Flexible Mesh User Manual 2D3D 2023*.

Didderen, K., van der Have, T. M., Bakker, E. G. R., & Japing, M. (2022). *Platte oester Waddenzee - Aanzet strategie en plan van aanpak voor herstel*. https://www.waddenzee.nl

Dijkema, K. S., Van Duin, W. E., Dijkman, E. M., Nicolai, A., Jongerius, H., Keegstra, H., & Jongsma, J. J. (2013). *Friese en Groninger kwelderwerken: Monitoring en beheer 1960-2010*. https://edepot.wur.nl/279715

Dijkstra, J. (2022). *Vegetation modelling tools*. Deltares. https://publicwiki.deltares.nl/display/VegMod/Vegetation+modelling+tools

Dissanayake, D. M. P. K., Ranasinghe, R., & Roelvink, J. A. (2012). The morphological response of large tidal inlet/basin systems to relative sea level rise. *Climatic Change*, *113*(2), 253–276. https://doi.org/10.1007/s10584-012-0402-z

Duarte, C. M., Losada, I. J., Hendriks, I. E., Mazarrasa, I., & Marbà, N. (2013). The role of coastal plant communities for climate change mitigation and adaptation. *Nature Climate Change*, *3*(11), 961–968. https://doi.org/10.1038/nclimate1970

Erftemeijer, P. L. A., Van Beek, J. K. L., Ochieng, C. A., Jager, Z., & Los, H. J. (2008). Eelgrass seed dispersal via floating generative shoots in the Dutch Wadden Sea: a model approach. *Marine Ecology Progress Series*, *358*, 115–124. https://doi.org/10.3354/meps07304

Familkhalili, R., & Tahvildari, N. (2022). Computational modeling of coupled waves and vegetation stem dynamics in highly flexible submerged meadows. *Advances in Water Resources*, *165*. https://doi.org/10.1016/j.advwatres.2022.104222

Fivash, G. S., Stüben, D., Bachmann, M., Walles, B., van Belzen, J., Didderen, K., Temmink, R. J. M., Lengkeek, W., van der Heide, T., & Bouma, T. J. (2021). Can we enhance ecosystem-based coastal defense by connecting oysters to marsh edges? Analyzing the limits of oyster reef establishment. *Ecological Engineering*, *165*. https://doi.org/10.1016/j.ecoleng.2021.106221

Fokker, P. A., Van Leijen, F. J., Orlic, B., Van Der Marel, H., & Hanssen, R. F. (2018). Subsidence in the Dutch Wadden Sea. *Netherlands Journal of Geosciences*, *97*(3), 129–181. https://doi.org/10.1017/njg.2018.9

Follett, E., Hays, C. G., & Nepf, H. (2019). Canopy-mediated hydrodynamics contributes to greater allelic richness in seeds produced higher in meadows of the coastal eelgrass Zostera marina. *Frontiers in Marine Science*, *6*. https://doi.org/10.3389/fmars.2019.00008

Govers, L. L., Heusinkveld, J. H. T., Gräfnings, M. L. E., Smeele, Q., & van der Heide, T. (2022). Adaptive intertidal seed-based seagrass restoration in the Dutch Wadden Sea. *PLOS ONE*, *17*(2). https://doi.org/10.1371/journal.pone.0262845

Govers, L., van der Heide, T., Smeele, Q., Huisinkveld, J., & van der Eijk, A. (2018). Stap voor stap ontrafelen van herstel groot zeegras. In *Natuur tijdschriften*. https://natuurtijdschriften.nl/pub/1010621/dln201811903001.pdf

Haasnoot, M., Kwadijk, J., Van Alphen, J., Le Bars, D., Van Den Hurk, B., Diermanse, F., Van Der Spek, A., Oude Essink, G., Delsman, J., & Mens, M. (2020). Adaptation to uncertain sea-level rise; how uncertainty in Antarctic mass-loss impacts the coastal adaptation strategy of the Netherlands. *Environmental Research Letters*, *15*(3), 034007. https://doi.org/10.1088/1748-9326/ab666c

Haines-Young, R., & Potschin, M. (2017). *Common International Classification of Ecosystem Services (CICES) - Guidance on the Application of the Revised Structure*. www.cices.eu

Hale, L., Meliane, I., Davidson, S., Sandwith, T., Beck, M., Hoekstra, J., Spalding, M., Murawski, S., Cyr, N., Osgood, K., Hatziolos, M., Van Eijck, P., Davidson, N., Eichbaum, W., Dreus, C., Obura, D., Tamelander, J., Herr, D., McClannen, C., & Marshall, P. (2009). Ecosystem-based adaptation in marine and coastal ecosystems. *Renewable Resources*, *4*, 21–28.

Hansen, J. C. R., & Reidenbach, M. A. (2012). Wave and tidally driven flows in eelgrass beds and their effect on sediment suspension. *Marine Ecology Progress Series*, *448*, 271–287. https://doi.org/10.3354/meps09225

He, F., Chen, J., Jiang, C., & Zhao, J. (2018). Effects of wave nonlinearity on wave attenuation by seagrass. *Haiyang Xuebao*, *40*(5), 24–36. https://doi.org/10.3969/j.isnn.0253-4193.2018.05.003

Hofstede, J. L. A., & Stock, M. (2018). Climate change adaptation in the Schleswig-Holstein sector of the Wadden Sea: an integrated state governmental strategy. *Journal of Coastal Conservation*, *22*(1), 199–207. https://doi.org/10.1007/S11852-016-0433-0

Horstman, E. M., Dohmen-Janssen, C. M., Bouma, T. J., & Hulscher, S. J. M. H. (2015). Tidal-scale flow routing and sedimentation in mangrove forests: Combining field data and numerical modelling. *Geomorphology*, *228*, 244–262. https://doi.org/10.1016/j.geomorph.2014.08.011

Jacobs, A. F. G., Heusinkveld, B. G., & Holtslag, A. A. M. (2008). Towards closing the surface energy budget of a mid-latitude grassland. *Boundary-Layer Meteorology*, *126*(1), 125–136. https://doi.org/10.1007/S10546-007-9209-2

Jacobs, P., Greeve, Y., Sikkema, M., Dubbeldam, M., & Philippart, C. J. M. (2020). Successful rearing of Ostrea edulis from parents originating from the Wadden Sea, the Netherlands. *Aquaculture Reports*, *18*. https://doi.org/10.1016/j.aqrep.2020.100537

Jordan, P., & Fröhle, P. (2022). Bridging the gap between coastal engineering and nature conservation? A review of coastal ecosystems as nature-based solutions for coastal protection. *Journal of Coastal Conservation*, *26*(2). https://doi.org/10.1007/S11852-021-00848-X

Karamouz, M., Asce, F., Heydari, Z., & Asce, S. M. (2020). Conceptual Design Framework for Coastal Flood Best Management Practices. *Journal of Water Resources Planning and Management*, *146*(6), 04020041. https://doi.org/10.1061/(asce)wr.1943-5452.0001224

Karamouz, M., Zoghi, A., & Mahmoudi, S. (2022). Flood Modeling in Coastal Cities and Flow through Vegetated BMPs: Conceptual Design. *Journal of Hydrologic Engineering*, *27*(10). https://doi.org/10.1061/(asce)he.1943-5584.0002206

Keyzer, L. M., Herman, P. M. J., Smits, B. P., Pietrzak, J. D., James, R. K., Candy, A. S., Riva, R. E. M., Bouma, T. J., van der Boog, C. G., Katsman, C. A., Slobbe, D. C., Zijlema, M., van Westen, R. M., & Dijkstra, H. A. (2020). The potential of coastal ecosystems to mitigate the impact of sea-level rise in shallow tropical bays. *Estuarine, Coastal and Shelf Science*, *246*, 107050. https://doi.org/10.1016/j.ecss.2020.107050

Kitsikoudis, V., Kibler, K. M., & Walters, L. J. (2020). In-situ measurements of turbulent flow over intertidal natural and degraded oyster reefs in an estuarine lagoon. *Ecological Engineering*, *143*. https://doi.org/10.1016/j.ecoleng.2019.105688

Klopstra, D., Barneveld, H. J., & Van Noortwijk, J. M. (1996). Analytical model for hydraulic roughness of submerged vegetation. *27th International IAHR Conference*, 775–780.

KNMI. (2021). *KNMI Klimaatsignaal '21 - Hoe het klimaat in Nederland snel verandert.*

Kobayashi, M., Watanabe, A., Furukawa, K., Tingson, K. N., & Habito, C. F. (2021). *Capitalizing on Co-Benefits and Synergies to Promote the Blue Economy in Asia and the Pacific - ADBI Working Paper Series*. Asian Development Bank Institute. https://www.adb.org/publications/capitalizing-co-benefits-synergies-promote-blue-economy-asia-and-pacific

Koch, E. W., Barbier, E. B., Silliman, B. R., Reed, D. J., Perillo, G. M. E., Hacker, S. D., Granek, E. F., Primavera, J. H., Muthiga, N., Polasky, S., Halpern, B. S., Kennedy, C. J., Kappel, C. V., & Wolanski, E. (2009). Non-linearity in ecosystem services: temporal and spatial variability in coastal protection. *Frontiers in Ecology and the Environment*, *7*(1), 29–37. https://doi.org/10.1890/080126

Kooi, H., Johnston, P., Lambeck, K., Smither, C., & Molendijk, R. (1998). Geological causes of recent (~100 yr) vertical land movement in the Netherlands. *Tectonophysics*, *299*(4), 297–316. https://doi.org/10.1016/S0040-1951(98)00209-1

Laugier, T., Rigollet, V., & De Casabianca, M. L. (1999). Seasonal dynamics in mixed eelgrass beds, Zostera marina L. and Z. noltii Hornem., in a Mediterranean coastal lagoon (Thau lagoon, France). *Aquatic Botany*, *63*(1), 51–69. https://doi.org/10.1016/S0304-3770(98)00105-3

Leonard, L. A., & Croft, A. L. (2006). The effect of standing biomass on flow velocity and turbulence in Spartina alterniflora canopies. *Estuarine, Coastal and Shelf Science*, *69*(3–4), 325–336. https://doi.org/10.1016/j.ecss.2006.05.004

Lokhorst, I. R., Braat, L., Leuven, J. R. F. W., Baar, A. W., Van Oorschot, M., Selaković, S., & Kleinhans, M. G. (2018). Morphological effects of vegetation on the tidal-fluvial transition in Holocene estuaries. *Earth Surface Dynamics*, *6*(4), 883–901. https://doi.org/10.5194/esurf-6-883-2018

Losada, I. J., Maza, M., & Lara, J. L. (2016). A new formulation for vegetation-induced damping under combined waves and currents. *Coastal Engineering*, *107*, 1–13. https://doi.org/10.1016/j.coastaleng.2015.09.011

Luhar, M., Coutu, S., Infantes, E., Fox, S., & Nepf, H. (2010). Wave-induced velocities inside a model seagrass bed. *Journal of Geophysical Research: Oceans*, *115*(12), 12005. https://doi.org/10.1029/2010JC006345

Manning, R. (1891). On the flow of water in open channels and pipes. *Institute of Civil Engineers of*

Ireland Transactions, *20*, 161–207.

Marijnissen, R., Esselink, P., Kok, M., Kroeze, C., & van Loon-Steensma, J. M. (2020). How natural processes contribute to flood protection - A sustainable adaptation scheme for a wide green dike. *Science of the Total Environment*, *739*. https://doi.org/10.1016/j.scitotenv.2020.139698

Maza, M., Lara, J., Ondiviela, B., & Losada, I. J. (2012). Wave attenuation modelling by submerged vegetation: ecolocial and engineering analysis. *Coastal Engineering Proceedings*, *1*(33), 62. https://doi.org/10.9753/icce.v33.management.62

Metzing, D. (2010). Global warming changes the terrestrial flora of the Wadden Sea. *Wadden Sea Ecosystem*, *26*, 211–216.

Moraes, R. P. L., Reguero, B. G., Mazarrasa, I., Ricker, M., & Juanes, J. A. (2022). Nature-Based Solutions in Coastal and Estuarine Areas of Europe. *Frontiers in Environmental Science*, *10*, 829526. https://doi.org/10.3389/fenvs.2022.829526

NAM. (2016). *Winningsplan Groningen 2016*. https://www.nam.nl/gas-en-olie/groningen-gasveld/winningsplan-groningen-gasveld.html

Natuurmonumenten. (n.d.). *Uithuizerwad - Natuurgebied*. Figure. Retrieved March 24, 2023, from https://www.natuurmonumenten.nl/natuurgebieden/uithuizerwad

Nehring, S., & Hesse, K. J. (2008). Invasive alien plants in marine protected areas: The Spartina anglica affair in the European Wadden Sea. *Biological Invasions*, *10*(6), 937–950. https://doi.org/10.1007/S10530-008-9244-Z

Nienhuis, P. H., & de bree, B. H. H. (1980). Production and growth dynamics of eelgrass (Zostera marina) in brackish lake grevelingen (The Netherlands). *Netherlands Journal of Sea Research*, *14*(1), 102–118. https://doi.org/10.1016/0077-7579(80)90016-2

Olesen, B., & Sand-Jensen, K. (1994). Demography of Shallow Eelgrass (Zostera Marina) Populations - Shoot Dynamics and Biomass Development. *The Journal of Ecology*, *82*(2), 379. https://doi.org/10.2307/2261305

Ondiviela, B., Losada, I. J., Lara, J. L., Maza, M., Galván, C., Bouma, T. J., & Van Belzen, J. (2014). The role of seagrasses in coastal protection in a changing climate. *Coastal Engineering*, *87*, 158–168. https://doi.org/10.1016/j.coastaleng.2013.11.005

Paul, M. (2018). The protection of sandy shores - Can we afford to ignore the contribution of seagrass? *Marine Pollution Bulletin*, *134*, 152–159. https://doi.org/10.1016/j.marpolbul.2017.08.012

Paul, M., & Amos, C. L. (2011). Spatial and seasonal variation in wave attenuation over Zostera noltii. *Journal of Geophysical Research: Oceans*, *116*(8). https://doi.org/10.1029/2010JC006797

Penning, E., Steetzel, H., Van Santen, R., de Lange, M., Ouwerkerk, S., Vuik, V., Fiselier, J., & de Vries, J. V. T. (2016). Establishing vegetated foreshores to increase dike safety along lake shores. *FLOODrisk 2016 - 3rd European Conference on Flood Risk Management*, *7*. https://doi.org/10.1051/e3sconf/20160712008

Pieterse, N., Knoop, J., Nabielek, K., Pols, L., & Tennekes, J. (2009). *Overstromingsrisicozonering in Nederland - Hoe in de ruimtelijke ordening met overstromingsrisico's kan worden omgegaan*. https://www.pbl.nl/publicaties/overstromingsrisicozonering-in-nederland

Pinsky, M. L., Guannel, G., & Arkema, K. K. (2013). Quantifying wave attenuation to inform coastal habitat conservation. *Ecosphere*, *4*(8), 1–16. https://doi.org/10.1890/ES13-00080.1

Polte, P., Schanz, A., & Asmus, H. (2005). The contribution of seagrass beds (Zostera noltii) to the function of tidal flats as a juvenile habitat for dominant, mobile epibenthos in the Wadden Sea. *Marine Biology*, *147*(3), 813–822. https://doi.org/10.1007/S00227-005-1583-Z

Pörtner, H. O., Roberts, D. C., Tignor, M., Alegría, A., Nicolai, M., Okem, A., Petzold, J., Rama, B., & Weye, N. M. (2019). Technical Summary. In H. O. Pörtner, D. C. Roberts, V. Masson-Delmotte, P. Zhai, M. Tignor, E. Poloczanska, K. Mintenbeck, A. Alegría, M. Nicolai, A. Okem, J. Petzold, B. Rama, & N. M. Weyer (Eds.), *IPCC Special Report on the Ocean and Cryosphere in a Changing Climate* (pp. 36–69). Cambridge University Press. https://doi.org/doi.org/10.1017/9781009157964.002

Reef, K. R. G., Lipari, G., Roos, P. C., & Hulscher, S. J. M. H. (2018). Time-varying storm surges on Lorentz's Wadden Sea networks. *Ocean Dynamics*, *68*(8), 1051–1065. https://doi.org/10.1007/S10236-018-1181-5

Rijkswaterstaat. (n.d.). *Contactformulier Servicedesk Data*. Retrieved November 23, 2022, from

https://www.rijkswaterstaat.nl/formulieren/contactformulier-servicedesk-data

Rodi, W. (1984). Turbulence models and their application in Hydraulics. In *Fundamentals of Division II: Experimental and Mathematical Fluid Dynamics*. Taylor & Francis.

Rozema, J., Leendertse, P., Bakker, J., & Van Wijnen, H. (2002). Nitrogen and Vegetation Dynamics in European Salt Marshes. *Concepts and Controversies in Tidal Marsh Ecology*, 469–491. https://doi.org/10.1007/0-306-47534-0_21

Salatin, R., Wang, H., Chen, Q., & Zhu, L. (2022). Assessing Wave Attenuation With Rising Sea Levels for Sustainable Oyster Reef-Based Living Shorelines. *Frontiers in Built Environment*, *8*, 92. https://doi.org/10.3389/fbuil.2022.884849

Schanz, A., & Asmus, H. (2003). Impact of hydrodynamics on development and morphology of intertidal seagrasses in the Wadden Sea. *Marine Ecology Progress Series*, *261*, 123–134. https://doi.org/10.3354/meps261123

Schoutens, K., Heuner, M., Minden, V., Schulte Ostermann, T., Silinski, A., Belliard, J. P., & Temmerman, S. (2019). How effective are tidal marshes as nature-based shoreline protection throughout seasons? *Limnology and Oceanography*, *64*(4), 1750–1762. https://doi.org/10.1002/lno.11149

Schrijvershof, R. A., van Maren, D. S., Torfs, P. J. J. F., & Hoitink, A. J. F. (2023). A Synthetic Spring-Neap Tidal Cycle for Long-Term Morphodynamic Models. *Journal of Geophysical Research: Earth Surface*, *128*(3). https://doi.org/10.1029/2022JF006799

Scyphers, S. B., Powers, S. P., Heck, K. L., & Byron, D. (2011). Oyster Reefs as Natural Breakwaters Mitigate Shoreline Loss and Facilitate Fisheries. *PLOS ONE*, *6*(8). https://doi.org/10.1371/journal.pone.0022396

Smaal, A. C., Kamermans, P., Have, T. M. van der, Engelsma, M. Y., & Sas, H. (2015). *Feasibility of Flat Oyster (Ostrea edulis L.) restoration in the Dutch part of the North Sea*.

Stancheva, M., Rangel-Buitrago, N., Anfuso, G., Palazov, A., Stanchev, H., & Correa, I. (2011). Expanding level of coastal armouring: Case studies from different countries. *Journal of Coastal Research*, *64*, 1815–1819.

Stronkhorst, J., Huisman, B., Giardino, A., Santinelli, G., & Santos, F. D. (2018). Sand nourishment strategies to mitigate coastal erosion and sea level rise at the coasts of Holland (The Netherlands) and Aveiro (Portugal) in the 21st century. *Ocean and Coastal Management*, *156*, 266–276. https://doi.org/10.1016/j.ocecoaman.2017.11.017

Temmerman, S., Bouma, T. J., Govers, G., Wang, Z. B., de Vries, M. B., & Herman, P. M. J. (2005). Impact of vegetation on flow routing and sedimentation patterns: Three-dimensional modeling for a tidal marsh. *Journal of Geophysical Research: Earth Surface*, *110*(4), 4019. https://doi.org/10.1029/2005JF000301

Temmerman, S., Meire, P., Bouma, T. J., Herman, P. M. J., Ysebaert, T., & de Vriend, H. J. (2013). Ecosystem-based coastal defence in the face of global change. *Nature*, *504*(7478), 79–83. https://doi.org/10.1038/nature12859

Thomas, S., Collins, K., Hauton, C., & Jensen, A. (2022). A Review of the Ecosystem Services Provided by the Native Oyster (Ostrea edulis): Implications for Restoration. *IOP Conference Series: Materials Science and Engineering*, *1245*(1). https://doi.org/10.1088/1757-899X/1245/1/012010

Twomey, A. J., Callaghan, D. P., O'Brien, K. R., & Saunders, M. I. (2022). Contextualising shoreline protection by seagrass using lessons from submerged breakwaters. *Estuarine, Costal and Shelf Science*, *276*(108011). https://doi.org/10.1016/j.ecss.2022.108011

Twomey, A. J., O'Brien, K. R., Callaghan, D. P., & Saunders, M. I. (2020). Synthesising wave attenuation for seagrass: Drag coefficient as a unifying indicator. *Marine Pollution Bulletin*, *160*. https://doi.org/10.1016/j.marpolbul.2020.111661

Valle, M. (2014). *Seagrass meadows under a changing climate: habitat modelling, restoration and monitoring*. Thesis - Universitad del Pais Vasco.

van der Nat, A., Vellinga, P., Leemans, R., & van Slobbe, E. (2016). Ranking coastal flood protection designs from engineered to nature-based. *Ecological Engineering*, *87*, 80–90. https://doi.org/10.1016/j.ecoleng.2015.11.007

van Katwijk, M. M., & Hermus, D. C. R. (2000). Effects of water dynamics on Zostera marina: transplantation experiments in the intertidal Dutch Wadden Sea. *Marine Ecology Progress*

Series, *208*, 107–118. https://doi.org/10.3354/meps208107

van Katwijk, M. M., Thorhaug, A., Marbà, N., Orth, R. J., Duarte, C. M., Kendrick, G. A., Althuizen, I. H. J., Balestri, E., Bernard, G., Cambridge, M. L., Cunha, A., Durance, C., Giesen, W., Han, Q., Hosokawa, S., Kiswara, W., Komatsu, T., Lardicci, C., Lee, K. S., … Verduin, J. J. (2016). Global analysis of seagrass restoration: the importance of large-scale planting. *Journal of Applied Ecology*, *53*(2), 567–578. https://doi.org/10.1111/1365-2664.12562

van Leeuwen, B. (2008). *Modeling mussel bed influence on fine sediment dynamics on a Wadden Sea intertidal flat*. Thesis - University of Twente.

van Loon-Steensma, J. M. (2015). Salt marshes to adapt the flood defences along the Dutch Wadden Sea coast. *Mitigation and Adaptation Strategies for Global Change*, *20*(6), 929–948. https://doi.org/10.1007/S11027-015-9640-5

van Prooijen, B. C., Tissier, M. F. S., De Wit, F. P., Pearson, S. G., Brakenhoff, L. B., Van Maarseveen, M. C. G., Van Der Vegt, M., Mol, J. W., Kok, F., Holzhauer, H., Van Der Werf, J. J., Vermaas, T., Gawehn, M., Grasmeijer, B., Elias, E. P. L., Tonnon, P. K., Santinelli, G., Antolínez, J. A. A., De Vet, P. L. M., … De Looff, H. (2020). Measurements of hydrodynamics, sediment, morphology and benthos on Ameland ebb-tidal delta and lower shoreface. *Earth System Science Data*, *12*(4), 2775–2786. https://doi.org/10.5194/essd-12-2775-2020

van Slobbe, E., de Vriend, H. J., Aarninkhof, S., Lulofs, K., de Vries, M., & Dircke, P. (2013). Building with Nature: In search of resilient storm surge protection strategies. *Natural Hazards*, *65*(1), 947–966. https://doi.org/10.1007/s11069-012-0342-y

van Veelen, T., Karunarathna, H., Bennett, W., Fairchild, T., & Reeve, D. E. (2019). Sensitivity of estuary hydrodynamics to vegetation parameterisation. *4th IMA International Conference On Flood Risk*.

Vermeersen, B. L. A., Slangen, A. B. A., Gerkema, T., Baart, F., Cohen, K. M., Dangendorf, S., Duran-Matute, M., Frederikse, T., Grinsted, A., Hijma, M. P., Jevrejeva, S., Kiden, P., Kleinherenbrink, M., Meijles, E. W., Palmer, M. D., Rietbroek, R., Riva, R. E. M., Schulz, E., Slobbe, D. C., … Van Der Wegen, M. (2018). Sea-level change in the Dutch Wadden Sea. *Netherlands Journal of Geosciences*, *97*(3), 79–127. https://doi.org/10.1017/njg.2018.7

Vuik, V., Suh Heo, H. Y., Zhu, Z., Borsje, B. W., & Jonkman, S. N. (2018). Stem breakage of salt marsh vegetation under wave forcing: A field and model study. *Estuarine, Coastal and Shelf Science*, *200*, 41–58. https://doi.org/10.1016/j.ecss.2017.09.028

Walles, B., Salvador de Paiva, J., van Prooijen, B. C., Ysebaert, T., & Smaal, A. C. (2015). The Ecosystem Engineer Crassostrea gigas Affects Tidal Flat Morphology Beyond the Boundary of Their Reef Structures. *Estuaries and Coasts*, *38*(3), 941–950. https://doi.org/10.1007/S12237-014-9860-Z

Walles, B., Troost, K., van den Ende, D., Nieuwhof, S., Smaal, A. C., & Ysebaert, T. (2016). From artificial structures to self-sustaining oyster reefs. *Journal of Sea Research*, *108*, 1–9. https://doi.org/10.1016/j.seares.2015.11.007

Walsh, C. (2018). Metageographies of coastal management: Negotiating spaces of nature and culture at the Wadden Sea. *Area*, *50*(2), 177–185. https://doi.org/10.1111/area.12404

Wang, Z. B., Elias, E. P. L., Van Der Spek, A. J. F., & Lodder, Q. J. (2018). Sediment budget and morphological development of the Dutch Wadden Sea: impact of accelerated sea-level rise and subsidence until 2100. *Netherlands Journal of Geosciences*, *97*(3), 183–214. https://doi.org/10.1017/njg.2018.8

Widdows, J., Pope, N. D., Brinsley, M. D., Asmus, H., & Asmus, R. M. (2008). Effects of seagrass beds (Zostera noltii and Z. marina) on near-bed hydrodynamics and sediment resuspension. *Marine Ecology Progress Series*, *358*, 125–136. https://doi.org/10.3354/meps07338

Willemsen, P. W. J. M., Smits, B. P., Borsje, B. W., Herman, P. M. J., Dijkstra, J. T., Bouma, T. J., & Hulscher, S. J. M. H. (2022). Modeling Decadal Salt Marsh Development: Variability of the Salt Marsh Edge Under Influence of Waves and Sediment Availability. *Water Resources Research*, *58*(1). https://doi.org/10.1029/2020wr028962

Wolff, W. J. (2005). Non-indigenous marine and estuarine species in The Netherlands. *Zoologische Mededelingen Leiden*, *79*, 1–116. https://repository.naturalis.nl/pub/210096

Wong, P. P., Losada, I. J., Gattuso, J.-P., Hinkel, J., Khattabi, A., McInnes, K. L., Saito, Y., Sallenger, A., Nicholls, R. J., Santos, F., Amez, S., Losada, I, Gattuso, J., Hinkel, J., Khattabi, A.,

McInnes, K., Saito, Y., Sallenger, A., Barros, V., … Levy, A. (2014). Coastal Systems and Low-Lying Areas. In C. B. Field, V. R. Barros, D. J. Dokken, K. J. Mach, M. D. Mastrandrea, T. E. Bilir, M. Chatterjee, K. L. Ebi, Y. O. Estrada, R. C. Genova, B. Girma, E. S. Kissel, A. N. Levy, S. MacCracken, P. R. Mastrandrea, & L. L. White (Eds.), *IPCC: Climate Change 2014: Impacts, Adaptation, and Vulnerability* (pp. 361–409). Cambridge university press.

Ysebaert, T., Walles, B., Haner, J., & Hancock, B. (2018). Habitat modification and coastal protection by ecosystem-engineering reef-building bivalves. In A. C. Smaal (Ed.), *Goods and Services of Marine Bivalves* (pp. 253–273). Springer International Publishing. https://doi.org/10.1007/978-3-319-96776-9_13

Zeiler, M., Milbradt, P., Plüß, A., & Valerius, J. (2014). Modelling Large Scale Sediment Transport in the German Bight (North Sea). *Die Küste*, *81*, 369–392. https://hdl.handle.net/20.500.11970/101701

Zeller, R. B., Weitzman, J. S., Abbett, M. E., Zarama, F. J., Fringer, O. B., & Koseff, J. R. (2014). Improved parameterization of seagrass blade dynamics and wave attenuation based on numerical and laboratory experiments. *Limnology and Oceanography*, *59*(1), 251–266. https://doi.org/10.4319/lo.2014.59.1.0251

Zhu, Z., Vuik, V., Visser, P. J., Soens, T., van Wesenbeeck, B., van de Koppel, J., Jonkman, S. N., Temmerman, S., & Bouma, T. J. (2020). Historic storms and the hidden value of coastal wetlands for nature-based flood defence. *Nature Sustainability*, *3*(10), 853–862. https://doi.org/10.1038/S41893-020-0556-Z

Zijl, F., Laan, S., & Groenenboom, J. (2021). *Development of a 3D model for the NW European Shelf (3D DCSM-FM)*.

Zipperle, A. M., Coyer, J. A., Reise, K., Stam, W. T., & Olsen, J. L. (2009). Evidence for persistent seed banks in dwarf eelgrass Zostera noltii in the German Wadden Sea. *Marine Ecology Progress Series*, *380*, 73–80. https://doi.org/10.3354/meps07929

Appendices

Appendix A. Additional Figures
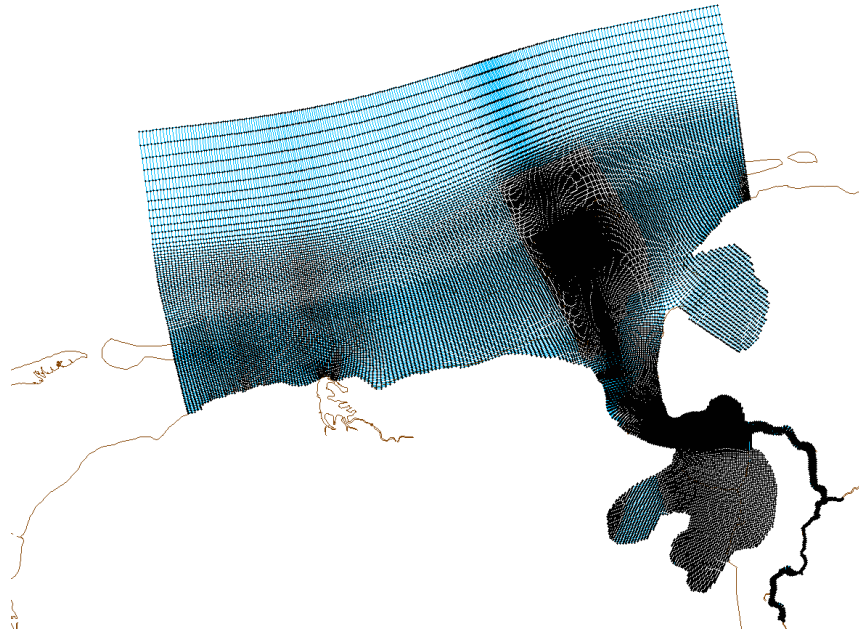
Figure A 1. Grid cells used in the Delft3D-FM Flow model with varying sizes, 1 km offshore to 30 m upstream the Ems river.
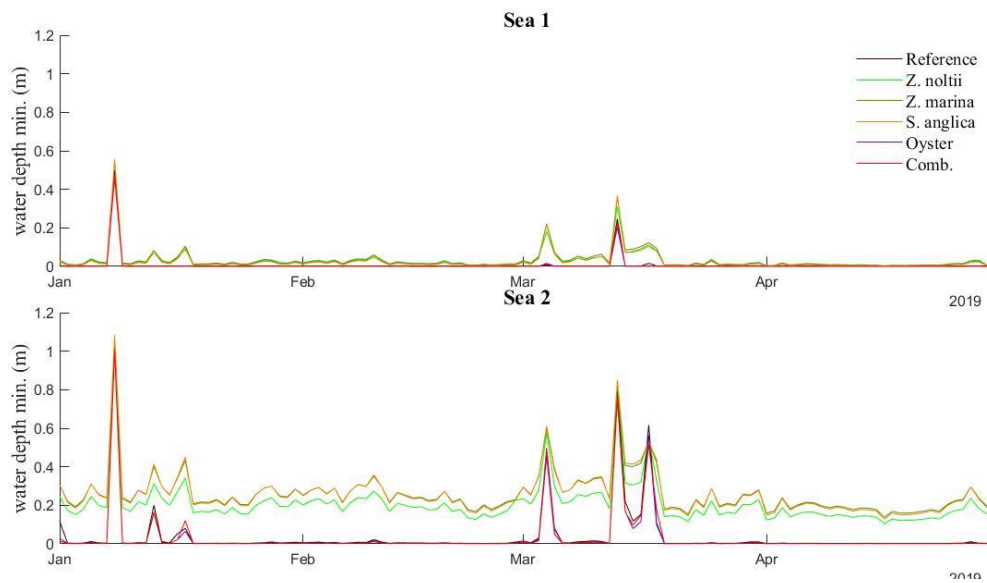
Figure A 2. Daily minimum water depth (m) levels at observation locations in the sea for the different NbS from January till May 2019.
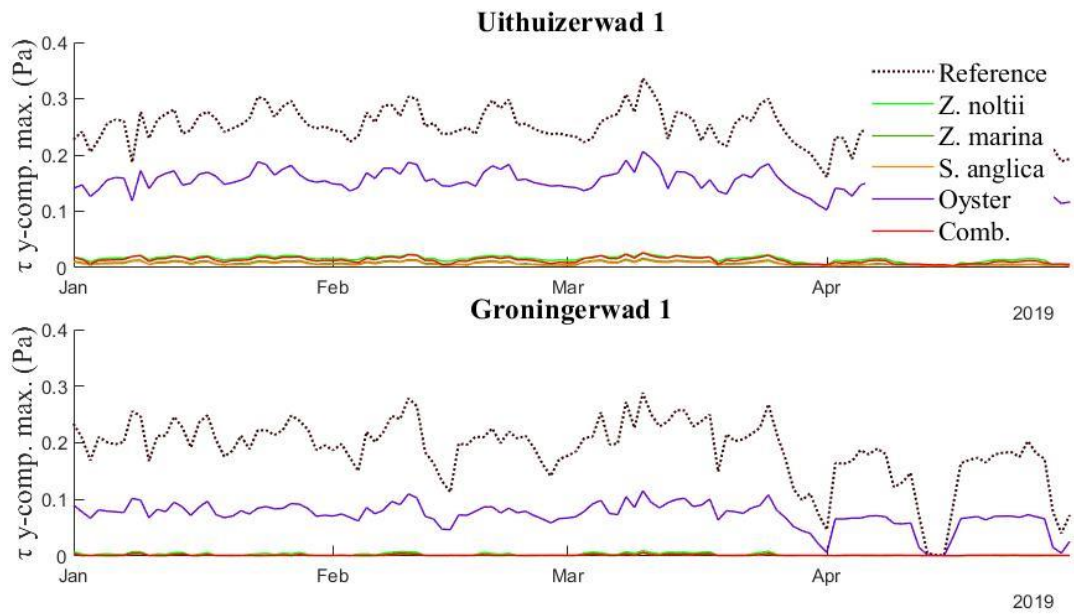
Figure A 3. Daily maximum bed shear stress (Pa) values for the y-component for the different NbS at the coastal observation points from January till May 2019.
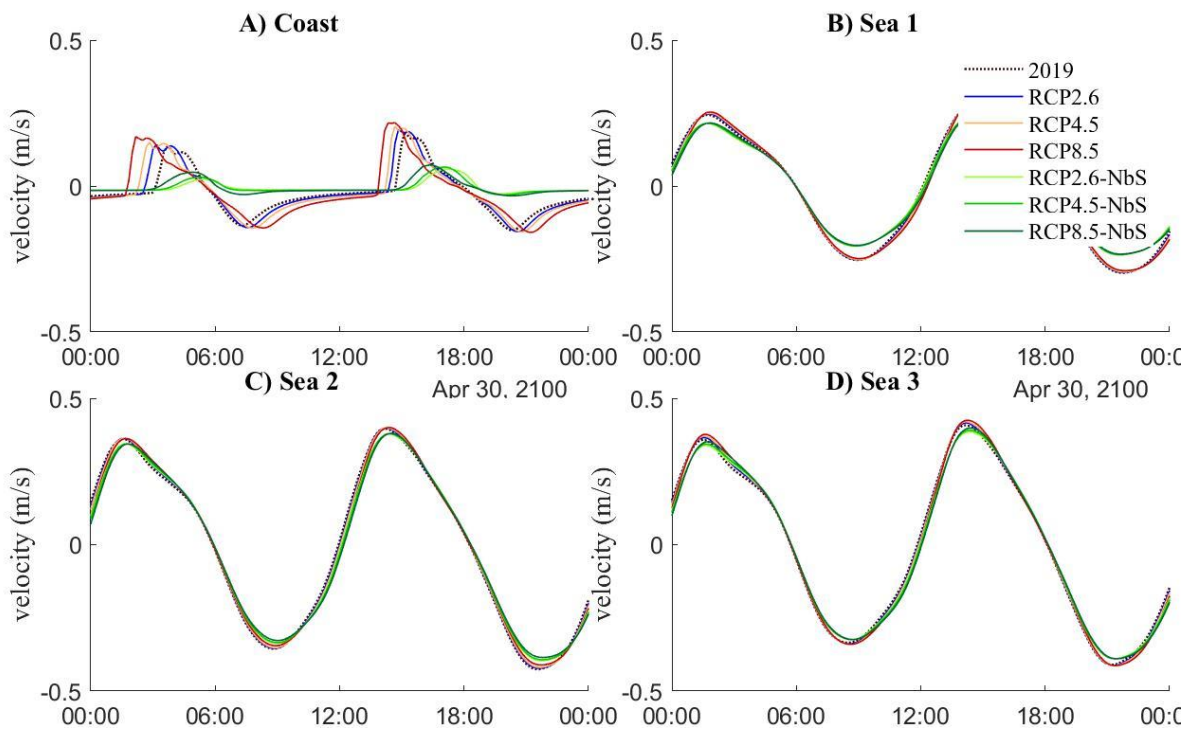
Figure A 4. Flow velocity (m s^{-1}) for the different scenarios with and without NbS at the cross sections in the study area on the 30th of April 2100.
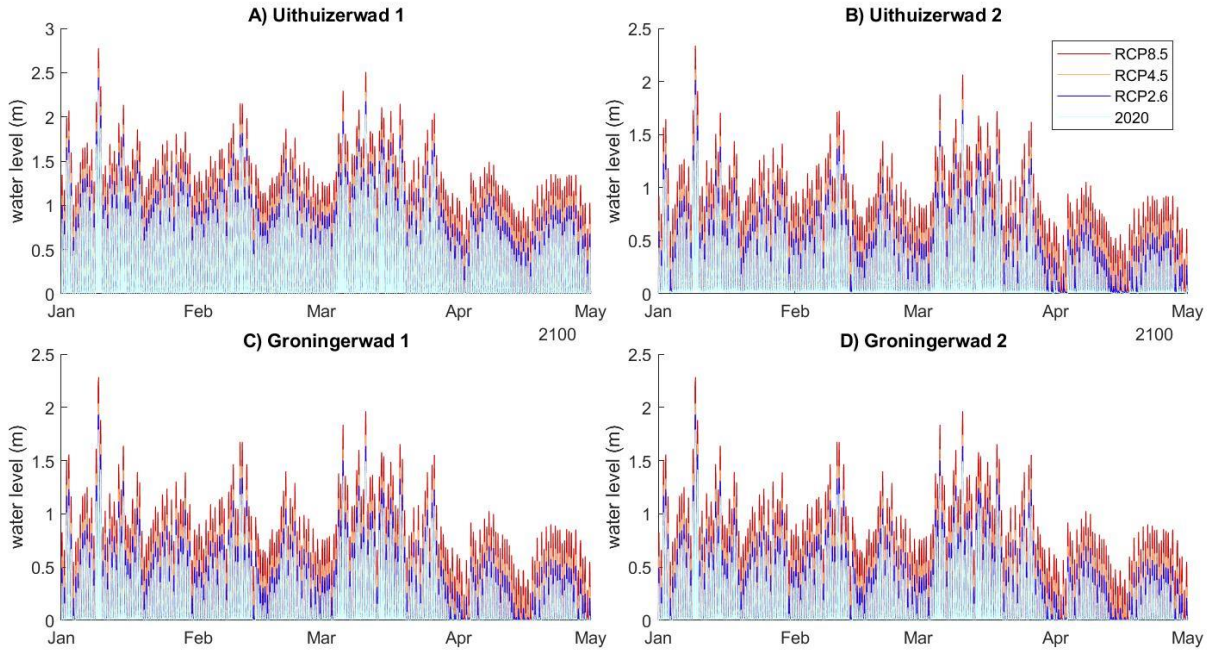
Figure A 5. Water depth level (m) for the different RCP SLR scenarios at the coastal observation points from January till May 2100.

Appendix B. Additional Tables

Table B 1. List of symbols used for different variables in this study with their units

Symbol	Name	Units
h_v	Height of NbS	m
p	Shoot or oyster density	m^{-2}
m	Leaves per shoot	[-]
D	Leaf or oyster diameter	m
n	Density	m^{-2}
C_d	Drag coefficient	[-]
C_b	Chèzy background bed roughness	$m^{0.5} s^{-1}$
C	Baptist roughness predictor	[-]
g	Gravitational acceleration	$m^3 kg^{-1}$
κ	Von Kármán constant	[-]
λ	Flow resistance coefficient of the NbS	[-]
f_i	Surface area fraction of the NbS	[-]
Q	Overall flow	$m s^{-1}$
t	Time	s
h	Water depth	m
U, V	Depth averaged velocity in x- and y-direction	$m s^{-1}$
u, v, w	Velocity components in x-, y- and z-directions	$m s^{-1}$
v_v	Vertical eddy viscosity coefficient	$m s^{-1}$
p_0	Initial density of the fluid	$kg\ m^{-3}$
p_d	Density of the fluid	$kg\ m^{-3}$
P	Pressure	Pa
M_x, M_y	External sources and sink of momentum	s^{-1}
F_x, F_y	Forces representing the unbalance of horizontal Reynold stresses	Pa
q_{in}, q_{out}	Local sources and sinks of water	s^{-1}
pd	Density of liquid	$g\ m\ L^{-1}$
g	Gravitational acceleration	$m^3\ kg^{-1}$
n_m	Manning's roughness coefficient	$m^{1/3}\ s^{-1}$
R	Hydraulic radius	-
τ	Bed shear stress	Pa

Table B 2. Parameters used for the different sensitivity runs, with different height (h_v), density (n), drag coefficient (C_d) of NbS and background roughness (C_b) values.

	h_v	n	C_d	C_b
ref	0.5	25	1	83
hv1	0.25	25	1	83
hv2	0.75	25	1	83
hv3	1	25	1	83
n1	0.5	1	1	83
n2	0.5	10	1	83
n3	0.5	50	1	83
n4	0.5	100	1	83

n5	0.5	1000	1	83
Cd1	0.5	25	0.5	83
Cd2	0.5	25	1	83
Cd3	0.5	25	1.5	83
Cd4	0.5	25	2	83
Cb1	0.5	25	1	1
Cb2	0.5	25	1	30
Cb3	0.5	25	1	60
Cb4	0.5	25	1	90

Table B 3. Mean peak velocity (m s^{-1}) standard deviations for the different NbS at the cross sections from January till May 2100.

Mean	Reference	S. anglica	Z. marina	Z. noltii	Oyster	Combined
Coast	0.041	0.017	0.017	0.020	0.038	0.017
Sea 1	0.067	0.038	0.035	0.034	0.061	0.056
Sea 2	0.101	0.079	0.074	0.073	0.098	0.097
Sea 3	0.102	0.078	0.073	0.072	0.098	0.093

Table B 4. Water depth (m) daily maximum peak values mean and standard deviation for the different NbS at the observation points from January till May 2019.

Mean	Reference	S. anglica	Z. marina	Z. noltii	Oyster	Combined
Uithuizerwad 1	1.055	0.988	0.936	0.915	0.995	1.026
Uithuizerwad 2	0.637	0.499	0.417	0.398	0.583	0.503
Groningerwad 1	0.594	0.489	0.415	0.397	0.546	0.450
Groningerwad 2	0.594	0.489	0.415	0.397	0.546	0.450
Sea 1	1.481	1.459	1.446	1.441	1.427	1.431
Sea 2	1.982	1.965	1.954	1.951	1.929	1.936
Standard deviation						
Uithuizerwad 1	0.371	0.392	0.432	0.445	0.370	0.401
Uithuizerwad 2	0.361	0.437	0.448	0.449	0.361	0.434
Groningerwad 1	0.348	0.406	0.424	0.425	0.347	0.413
Groningerwad 2	0.348	0.406	0.424	0.425	0.347	0.413
Sea 1	0.380	0.380	0.380	0.381	0.379	0.377
Sea 2	0.397	0.389	0.387	0.387	0.396	0.393

Table B 5. Water depth (m) daily minimum peak values mean and standard deviation for the different NbS at the observation points from January till May 2019.

Mean	Reference	S. anglica	Z. marina	Z. noltii	Oyster	Combined
Uithuizerwad 1	0.003	0.137	0.149	0.129	0.002	0.157
Uithuizerwad 2	0.013	0.075	0.062	0.053	0.009	0.073
Groningerwad 1	0.006	0.055	0.047	0.038	0.004	0.047
Groningerwad 2	0.006	0.055	0.047	0.038	0.004	0.047
Sea 1	0.007	0.029	0.033	0.027	0.006	0.006
Sea 2	0.036	0.208	0.260	0.257	0.030	0.032
Standard deviation						
Uithuizerwad 1	0.002	0.045	0.068	0.071	0.001	0.053
Uithuizerwad 2	0.005	0.048	0.052	0.048	0.004	0.046
Groningerwad 1	0.003	0.050	0.057	0.052	0.002	0.051

Groningerwad 2	0.003	0.050	0.057	0.052	0.002	0.051
Sea 1	0.049	0.058	0.063	0.063	0.044	0.046
Sea 2	0.136	0.118	0.117	0.121	0.127	0.129

Table B 6. Daily maximum bed shear stress (Pa) mean and standard deviation in the x-direction for the different NbS at the observation points from January till May 2019.

Mean	Reference	S. anglica	Z. marina	Z. noltii	Oyster	Combined
Uithuizerwad 1	0.142	0.028	0.023	0.022	0.086	0.027
Uithuizerwad 2	0.037	0.001	0.001	0.001	0.012	0.001
Groningerwad 1	0.375	0.010	0.005	0.004	0.109	0.005
Groningerwad 2	0.375	0.010	0.005	0.004	0.109	0.005
Sea 1	0.102	0.007	0.004	0.004	0.037	0.055
Sea 2	0.201	0.007	0.004	0.004	0.061	0.027
Standard deviation						
Uithuizerwad 1	0.054	0.012	0.011	0.011	0.035	0.009
Uithuizerwad 2	0.019	0.001	0.001	0.001	0.007	0.002
Groningerwad 1	0.186	0.013	0.008	0.007	0.060	0.009
Groningerwad 2	0.186	0.013	0.008	0.007	0.060	0.009
Sea 1	0.042	0.004	0.003	0.003	0.018	0.016
Sea 2	0.069	0.002	0.001	0.001	0.021	0.010

Table B 7. Daily maximum bed shear stress (Pa) mean and standard deviation in the y-direction for the different NbS at the observation points from January till May 2019.

Mean	Reference	S. anglica	Z. marina	Z. noltii	Oyster	Combined
Uithuizerwad 1	0.247	0.016	0.008	0.007	0.152	0.013
Uithuizerwad 2	0.018	0.000	0.000	0.000	0.007	0.000
Groningerwad 1	0.188	0.003	0.002	0.002	0.072	0.002
Groningerwad 2	0.188	0.003	0.002	0.002	0.072	0.002
Sea 1	0.071	0.006	0.004	0.003	0.033	0.018
Sea 2	0.260	0.012	0.008	0.007	0.069	0.025
Standard deviation						
Uithuizerwad 1	0.038	0.005	0.003	0.002	0.022	0.005
Uithuizerwad 2	0.011	0.001	0.000	0.000	0.005	0.000
Groningerwad 1	0.057	0.002	0.001	0.001	0.023	0.001
Groningerwad 2	0.057	0.002	0.001	0.001	0.023	0.001
Sea 1	0.035	0.002	0.001	0.001	0.013	0.003
Sea 2	0.060	0.002	0.002	0.001	0.015	0.012

Table B 8. Maximum daily flow velocity (m s^{-1}) mean and standard deviation for the different scenarios at the cross sections. For the reference model from January till May 2019 and the scenarios the same months in 2100.

Mean	Ref.	RCP2.6	RCP4.5	RCP8.5	RCP2.6-nbs	RCP4.5-nbs	RCP8.5-nbs
Coast	0.24	0.25	0.26	0.27	0.08	0.08	0.09
Sea 1	0.34	0.34	0.34	0.34	0.29	0.29	0.29
Sea 2	0.50	0.50	0.50	0.50	0.47	0.47	0.47
Sea 3	0.53	0.53	0.54	0.54	0.49	0.49	0.50

Standard deviation							
Coast	0.04	0.04	0.05	0.05	0.02	0.02	0.02
Sea 1	0.07	0.07	0.07	0.07	0.06	0.06	0.06
Sea 2	0.10	0.10	0.10	0.11	0.10	0.10	0.10
Sea 3	0.10	0.10	0.11	0.11	0.10	0.10	0.10

Table B 9. Maximum daily water depth (m) mean and standard deviation for the different scenarios at the cross sections. For the reference model from January till May 2019 and the scenarios the same months in 2100.

Mean	Ref.	RCP2.6	RCP4.5	RCP8.5	RCP2.6-nbs	RCP4.5-nbs	RCP8.5-nbs
Uithuizerwad 1	1.06	1.21	1.31	1.55	1.19	1.31	1.55
Uithuizerwad 2	0.64	0.79	0.89	1.13	0.68	0.83	1.11
Groningerwad 1	0.59	0.74	0.85	1.08	0.62	0.76	1.05
Groningerwad 2	0.59	0.74	0.85	1.08	0.62	0.76	1.05
Standard deviation							
Uithuizerwad 1	0.01	0.01	0.01	0.01	0.08	0.10	0.15
Uithuizerwad 2	0.01	0.01	0.01	0.01	0.08	0.10	0.15
Groningerwad 1	0.01	0.01	0.01	0.01	0.08	0.10	0.15
Groningerwad 2	0.01	0.01	0.01	0.01	0.08	0.10	0.15

Table B 10. Average daily maximum and minimum water depth (m) and velocity (m s^{-1}) for different NbS height values (H_v) with standard deviation (SD) for 1-10 January 2019. The water depth was measured at the Uithuizerwad 2 observation point and the velocity at the whole coast of the study area.

Water depth	No NbS	$h_v=0.25$	$h_v=0.5$	$h_v=0.75$	$h_v=1$
Max.	0.926	0.782	0.660	0.555	0.426
Min.	0.015	0.085	0.078	0.072	0.037
Max. SD.	0.413	0.546	0.603	0.598	0.606
Min. SD.	0.006	0.043	0.070	0.088	0.032
Velocity					
Max.	0.268	0.098	0.071	0.049	0.033
Min.	-0.162	-0.038	-0.019	-0.012	-0.012
Max. SD.	0.029	0.017	0.017	0.022	0.023
Min. SD.	0.011	0.035	0.032	0.019	0.010

Table B 11. Average daily maximum and minimum water depth (m) and velocity (m s^{-1}) for different NbS density (n) values with standard deviation (SD) for 1-10 January 2019. The water depth was measured at the Uithuizerwad 2 observation point and the velocity at the whole coast of the study area.

Water depth	No NbS	n=1	n=10	n=25	n=50	n=100	n=1000
Max.	0.926	0.779	0.676	0.660	0.660	0.665	0.711
Min.	0.015	0.022	0.052	0.078	0.102	0.130	0.248
Max. SD.	0.413	0.547	0.597	0.603	0.601	0.596	0.556
Min. SD.	0.006	0.017	0.052	0.070	0.082	0.091	0.096
Velocity							
Max.	0.268	0.117	0.081	0.071	0.064	0.059	0.044
Min.	-0.162	-0.055	-0.023	-0.019	-0.018	-0.017	-0.017

Max. SD.	0.029	0.019	0.016	0.017	0.018	0.018	0.020
Min. SD.	0.011	0.047	0.037	0.032	0.030	0.027	0.020

Table B 12. Average daily maximum and minimum water depth (m) and velocity (m s^{-1}) for different drag coefficient values (C$_d$) with standard deviation (SD) for 1-10 January 2019. The water depth was measured at the Uithuizerwad 2 observation point and the velocity at the whole coast of the study area.

Water depth					
	No NbS	*C$_d$=0.5*	*C$_d$=1*	*C$_d$=1.5*	*C$_d$=2*
Max.	0.926	0.671	0.660	0.659	0.660
Min.	0.015	0.057	0.078	0.091	0.102
Max. SD.	0.413	0.599	0.603	0.603	0.601
Min. SD.	0.006	0.056	0.070	0.077	0.082
Velocity					
Max.	0.268	0.079	0.071	0.067	0.064
Min.	-0.162	-0.022	-0.019	-0.018	-0.018
Max. SD.	0.029	0.017	0.017	0.017	0.018
Min. SD.	0.011	0.035	0.032	0.031	0.030

Table B 13. Average daily maximum and minimum water depth (m) and velocity (m s^{-1}) for different background roughness values (C$_b$) with standard deviation (SD) for 1-10 January 2019. The water depth was measured at the Uithuizerwad 2 observation point and the velocity at the whole coast of the study area.

Water depth						
	No NbS	*C$_b$=1*	*C$_b$=30*	*C$_b$=60*	*C$_b$=83*	*C$_b$=90*
Max.	0.926	0.680	0.661	0.660	0.660	0.660
Min.	0.015	0.145	0.078	0.078	0.078	0.078
Max. SD.	0.413	0.586	0.603	0.603	0.603	0.603
Min. SD.	0.006	0.079	0.070	0.070	0.070	0.070
Velocity						
Max.	0.268	0.060	0.071	0.071	0.071	0.071
Min.	-0.162	-0.018	-0.019	-0.019	-0.019	-0.019
Max. SD.	0.029	0.019	0.017	0.017	0.017	0.017
Min. SD.	0.011	0.027	0.032	0.032	0.032	0.032

Appendix C. Flow module equations

The continuity equation assumes mass conservation within the system. This means that there is an integration of the flow over the total depth, considering the kinematic boundary conditions at the water surface and the bed level (Eq. 16).

$$Q = \frac{\partial h}{\partial t} + \frac{\partial Uh}{\partial x} + \frac{\partial Vh}{\partial y} \qquad \qquad Eq.\ 15$$

where Q is the overall flow (m s^{-1}), t is time (s), h is the water depth (m), U and V are the depth averaged velocities (m s^{-1}), and x and y are the directions.

For the momentum equation in horizontal directions the Navier-stokes equations are used for an incompressible fluid. For these equations, the shallow water assumption and the Boussinesq assumption are made. The shallow water assumption is made because the depth is assumed to be much smaller than the horizontal scale of length (Deltares, 2022). The Boussinesq assumption is made as the variable density is only taken into account in the pressure term (Deltares, 2022). The following equations in x and y directions are used:

$$\frac{\partial u}{\partial t} + u\frac{\partial u}{\partial x} + v\frac{\partial u}{\partial y} + w\frac{\partial u}{\partial z} - fv = -\frac{1}{p_0}\frac{\partial P}{\partial x} + F_x + \frac{\partial}{\partial z}\left(v_V\frac{\partial u}{\partial z}\right) + M_x \qquad Eq.\ 16$$

$$\frac{\partial u}{\partial t} + u\frac{\partial u}{\partial x} + v\frac{\partial u}{\partial y} + w\frac{\partial u}{\partial z} - fu = -\frac{1}{p_0}\frac{\partial P}{\partial y} + F_y + \frac{\partial}{\partial z}\left(v_V\frac{\partial u}{\partial z}\right) + M_y \qquad Eq.\ 17$$

u, v, w:	velocity components in x-, y- and z-directions (m s^{-1})
v_v:	vertical eddy viscosity coefficient (m s^{-1})
p_0:	initial density (kg m^{-3})
$\partial P/\partial x$, $\partial P/\partial y$:	pressure gradients with other density variations being neglected
F_x, F_y:	forces representing the unbalance of horizontal Reynold stresses (Pa)
M_x, M_y:	contribution of external sources or sinks of momentum (s^{-1})

Within the model the Reynold stresses are modelled with the eddy viscosity concept (Rodi, 1984) and were set to 0.1.

The vertical velocities were modelled with the transport equation for conservative constituents (Eq. 19).

$$\frac{\partial h}{\partial t} + \frac{\partial uh}{\partial x} + \frac{\partial vh}{\partial y} + \frac{\partial w}{\partial z} = h(q_{in} - q_{out}) \qquad \qquad Eq.\ 18$$

Where q_{in} and q_{out} are the local sources and sinks of water per unit of volume (s^{-1}). By making the shallow-water assumption it is assumed that the vertical accelerations are sufficiently small to be neglected. Consequently, the vertical momentum equation can be reduced to the hydrostatic pressure equation (Eq. 20).

$$\frac{\partial P}{\partial z} = -p_d gh \qquad \qquad Eq.\ 19$$

With P the pressure (Pa), p_d the density of the liquid (kg m^{-3}), g the gravitational acceleration (m^3 kg^{-1}) and h the water depth (m).

By elaborating the viscous stresses in the momentum equation and substituting the hydrostatic equation, the following equations can be derived (Willemsen et al., 2022):

$$\frac{\partial h}{\partial t} + \frac{\partial uh}{\partial x} + \frac{\partial vh}{\partial y} = 0 \qquad \qquad Eq.\ 20$$

$$\frac{\partial u}{\partial t} + u\frac{\partial u}{\partial x} + v\frac{\partial u}{\partial y} + g\frac{\partial h}{\partial x} - v + \frac{1}{p_0}\left(\frac{\partial \tau_{xx}}{\partial x} + \frac{\partial \tau_{xy}}{\partial y} + \frac{\partial \tau_{bx}}{h}\right) = 0 \qquad Eq.\ 21$$

$$\frac{\partial v}{\partial t} + u\frac{\partial v}{\partial x} + v\frac{\partial v}{\partial y} + g\frac{\partial h}{\partial y} - u + \frac{1}{p_0}\left(\frac{\partial \tau_{yx}}{\partial x} + \frac{\partial \tau_{yy}}{\partial y} + \frac{\partial \tau_{by}}{h}\right) = 0 \qquad\qquad Eq.\ 22$$

Where τ represents the bed shear stress in different directions.